



— BUREAU OF —
RECLAMATION

Uplift Pressure and Flow through Open Offset Joints in Spillway Chutes

**Science and Technology Program
Research and Development Office
Final Report ST-2021-19170-01**

**Technology Development Program
Dam Safety Office, Dam Safety and Infrastructure
Final Report DSO-2021-08**



REPORT DOCUMENTATION PAGE				Form Approved OMB No. 0704-0188	
<p>The public reporting burden for this collection of information is estimated to average 1 hour per response, including the time for reviewing instructions, searching existing data sources, gathering and maintaining the data needed, and completing and reviewing the collection of information. Send comments regarding this burden estimate or any other aspect of this collection of information, including suggestions for reducing the burden, to Department of Defense, Washington Headquarters Services, Directorate for Information Operations and Reports (0704-0188), 1215 Jefferson Davis Highway, Suite 1204, Arlington, VA 22202-4302. Respondents should be aware that notwithstanding any other provision of law, no person shall be subject to any penalty for failing to comply with a collection of information if it does not display a currently valid OMB control number.</p> <p>PLEASE DO NOT RETURN YOUR FORM TO THE ABOVE ADDRESS.</p>					
1. REPORT DATE (DD-MM-YYYY) 09-30-2021		2. REPORT TYPE Research		3. DATES COVERED (From - To) 2019-2021	
4. TITLE AND SUBTITLE Uplift Pressure and Flow through Open Offset Joints in Spillway Chutes			5a. CONTRACT NUMBER RR.4888FARD.1900601 / FA983		
			5b. GRANT NUMBER		
			5c. PROGRAM ELEMENT NUMBER 1541 (S&T)		
6. AUTHOR(S) Tony L. Wahl, P.E. Technical Specialist			5d. PROJECT NUMBER Final Report ST-2021-19170-01 / DSO-2021-08		
			5e. TASK NUMBER		
			5f. WORK UNIT NUMBER		
7. PERFORMING ORGANIZATION NAME(S) AND ADDRESS(ES) Hydraulic Investigations & Laboratory Services Group Technical Service Center Bureau of Reclamation Denver, CO 80225-0007			8. PERFORMING ORGANIZATION REPORT NUMBER ST-2021-19170-01 / DSO-2021-08		
9. SPONSORING/MONITORING AGENCY NAME(S) AND ADDRESS(ES) Science and Technology Program, Research and Development Office Technology Development Program, Dam Safety Office Bureau of Reclamation U.S. Department of the Interior PO Box 25007, Denver, CO 80225-0007			10. SPONSOR/MONITOR'S ACRONYM(S) Reclamation		
			11. SPONSOR/MONITOR'S REPORT NUMBER(S) Final Report ST-2021-19170-01 Final Report DSO-2021-08		
12. DISTRIBUTION/AVAILABILITY STATEMENT Final Report may be downloaded from https://www.usbr.gov/research/projects/index.html					
13. SUPPLEMENTARY NOTES					
14. ABSTRACT Hydraulic jacking has caused catastrophic spillway chute failures in recent years, including at Oroville Dam in 2017 and on the fifth drop structure of the St. Mary Canal on Reclamation's Milk River Project (Montana) in 2020. Void development beneath spillways is a frequent issue on Reclamation projects and hydraulic jacking failure modes are commonly considered in Reclamation risk analysis studies. This project reanalyzed laboratory tests performed ca. 1976 and 2007 to develop improved predictive relationships for uplift pressure at sealed joints (no foundation drainage) with varying geometries. Uplift pressures were related to mean channel velocity, estimated boundary layer velocities, and the dimensionless ratio of gap width to joint offset height. New laboratory testing performed in 2021 led to a better understanding of the role of boundary layer velocity profiles in the generation of uplift pressure and developed the first experimentally validated relationships for predicting flow rates through open joints. These findings will aid spillway designers and risk assessment teams considering spillway slab anchors and foundation drainage systems.					
15. SUBJECT TERMS Hydraulic jacking, spillway, uplift, boundary layer					
16. SECURITY CLASSIFICATION OF:			17. LIMITATION OF ABSTRACT	18. NUMBER OF PAGES 57	19a. NAME OF RESPONSIBLE PERSON Tony Wahl
a. REPORT U	b. ABSTRACT U	THIS PAGE U			19b. TELEPHONE NUMBER (Include area code) 303-445-2155

Mission Statements

The Department of the Interior (DOI) conserves and manages the Nation's natural resources and cultural heritage for the benefit and enjoyment of the American people, provides scientific and other information about natural resources and natural hazards to address societal challenges and create opportunities for the American people, and honors the Nation's trust responsibilities or special commitments to American Indians, Alaska Natives, and affiliated island communities to help them prosper.

The mission of the Bureau of Reclamation is to manage, develop, and protect water and related resources in an environmentally and economically sound manner in the interest of the American public.

Disclaimer

Information in this report may not be used for advertising or promotional purposes. The data and findings should not be construed as an endorsement of any product or firm by the Bureau of Reclamation, Department of Interior, or Federal Government. The products evaluated in the report were evaluated for purposes specific to the Bureau of Reclamation mission. Reclamation gives no warranties or guarantees, expressed or implied, for the products evaluated in this report, including merchantability or fitness for a particular purpose.

Acknowledgements

This research was jointly funded by the Bureau of Reclamation Research Office Science and Technology Program and the Dam Safety Office Technology Development Program.

Cover photos show chute failures at the fifth drop structure of the St. Mary Canal on Reclamation's Milk River Project (Montana) in 2020, and Oroville Dam (California) in 2017.

Uplift Pressure and Flow through Open Offset Joints in Spillway Chutes

Final Report ST-2021-19170-01

Final Report DSO-2021-08

prepared by

Technical Service Center

Tony L. Wahl, P.E., Technical Specialist

Peer Review

Bureau of Reclamation

**Science and Technology Program
Research and Development Office
Final Report ST-2021-19170-01**

**Technology Development Program
Dam Safety Office, Dam Safety and Infrastructure
Final Report DSO-2021-08**

Uplift Pressure and Flow through Open Offset Joints in Spillway Chutes

**Prepared by: Tony L. Wahl, P.E.
Technical Specialist, Hydraulic Investigations & Laboratory Services Group, 86-68560**

**Peer Review by: Bryan J. Heiner, P.E.
Hydraulic Engineer, Hydraulic Investigations & Laboratory Services Group, 86-68560**

**Technical Approval by: Connie Svoboda, P.E.
Acting Manager, Hydraulic Investigations & Laboratory Services Group, 86-68560**

"This information is distributed solely for the purpose of pre-dissemination peer review under applicable information quality guidelines. It has not been formally disseminated by the Bureau of Reclamation. It does not represent and should not be construed to represent Reclamation's determination or policy."

Contents

	Page
Executive Summary	ix
Introduction	1
Previous Research.....	1
Objectives.....	2
Limitations.....	2
Experimental Facility & Methods	3
Experimental Results.....	6
Uplift Pressures.....	6
Flow Rates Through Joints	10
Separately Published End Products	11
Project Data.....	12
References	12
Appendix A.....	13
Appendix B.....	14

Figures

Page

Figure 1. — Spillway uplift research flume.	4
Figure 2. — A jet box regulates the depth and velocity of incoming flow.....	4
Figure 3. — Flow attached to the flume floor as it flows over a small-height offset (left); Flow launched or detached from the floor by a large-height offset (right).....	4
Figure 4. — Pitot tube used to measure spillway chute velocity profile.....	5
Figure 5. — Flow exiting the flume through the simulated joint during testing of a partially vented condition. Several valves regulate the back-pressure and control the flow out of the chamber below the joint.	5
Figure 6. — Simulated spillway joint geometries for small (left) and large (right) β values.....	5
Figure 7. — Dimensionless flow velocity vs. dimensionless depth (aggregated data from all tests).	6
Figure 8. — Relations between observed uplift pressure ratios and the β ratio of simulated offsets. Boundary layer reference velocities are at 75% of the offset height (top), 50% of the offset height (middle), and 25% of the offset height (bottom).....	7
Figure 9. — Approximate power curve relation for the normalized stagnation streamline height.....	8
Figure 10. — Uplift pressure relations for paired high- and low-Froude number tests. The trend is similar to Figure 7 for changing values of the independent variable, $(Fr^*_v)\beta$	9
Figure 11. — Normalized stagnation height vs. $(Fr^*_v)\beta$	9
Figure 12. — Curve relating observed joint flow discharge coefficients to the velocity ratio at the joint entrance.	10
Figure 13. — Different and inconsistent relation between the discharge coefficient and the gap-to-channel velocity ratio for $\beta=0.55$ and $\beta=0.75$	11

Executive Summary

Hydraulic jacking occurs when high velocity flow in a spillway chute or similar structure passes over an open joint combined with an offset of the flow surface into the flow. The problem may be a joint in poor condition or shifted from its original alignment, a crack in a concrete slab, a damaged concrete surface (a spall) located adjacent to a joint, or a slab that has settled or heaved up over an extended area. Flow striking the offset is brought suddenly to rest (stagnation), creating high pressures at the floor of the channel that propagate through the opening and force flow into it. High pressure may extend under the slab for significant distances, especially if there are voids in the foundation below the slab. If pressures are high enough, total uplift forces capable of jacking the slab further up into the flow are possible. Additionally, flow through the slab may create or enlarge voids, progressively extending the area that can be affected by uplift pressure. Large uplift pressures and/or large voids can lead to explosive and catastrophic slab failures, followed by rapid erosion of underlying material. Many spillways and chutes are constructed on soil foundations, making this a widespread issue for the Bureau of Reclamation (Reclamation) and other water resources agencies. Engineers charged with the design of new facilities or the analysis of risks at existing facilities have had limited experimental data to support estimating uplift pressure loads. No accurate experimental data on flow rates through open joints has ever been obtained from laboratory testing.

Hydraulic jacking caused catastrophic chute failures at the Oroville Dam spillway in 2017 and on the 5th drop structure of the St. Mary Canal on the Milk River Project (Montana) in 2020. Hydraulic jacking was also responsible for failures at Reclamation's Big Sandy Dam (1983) and Dickinson Dam (1960s). Void development beneath spillways is a frequent issue on Reclamation projects and hydraulic jacking failure modes are commonly considered in Reclamation risk analysis studies. Recent examples include the spillway chutes at Hyrum Dam and Vallecito Dam. Hydraulic jacking may also occur in channels used for sediment bypass operations, which are lined with granite, basalt, or high-strength concrete panels to resist abrasion. Uplift may also play a role in the failure of tunnel and pipe linings provided for corrosion resistance and friction reduction.

This project has addressed hydraulic jacking in three ways. First, a literature review confirmed that the only experimental studies are those performed in Reclamation's hydraulics laboratory in 1976 and 2007. A second phase of the project took an in-depth look at these studies, reanalyzing the data from them in a dimensionless manner and reconciling issues that made it challenging to compare their results to one another. Boundary layer velocity profiles were estimated in these test facilities and relationships between uplift pressure and boundary layer conditions were developed, pursuing an idea proposed by the Oroville Dam Independent Forensic Team. Finally, the third phase of the project used new laboratory testing in 2021 to gain a better understanding of the role of boundary layer velocity profiles in the generation of uplift pressure and developed the first experimentally validated relationships for predicting flow rates through open joints. These findings will aid spillway designers and risk assessment teams considering spillway slab anchors, foundation drainage systems, and probabilities of failure due to hydraulic jacking failure modes.

Introduction

Hydraulic jacking occurs when high velocity flow in a spillway chute or similar structure passes over a defect in the chute lining. The defect could be a joint in poor condition or shifted from its original alignment, a crack in the slab, a damaged zone of the concrete surface (a spall) located adjacent to a joint, or a slab that has settled or heaved up over an extended area. The problem becomes severe when the defect creates an offset of the flow surface into the flow adjacent to an opening such as an unsealed joint or displaced crack. High velocity flow striking the offset is brought suddenly to rest (stagnation), creating high pressures at the floor of the channel that propagate through the crack and force flow into it. The high pressure may extend under the slab for significant distances, especially if there are voids in the foundation below the slab. If pressures are high enough, total uplift forces capable of jacking the slab further up into the flow are possible. Additionally, flow through the slab may create or enlarge voids, progressively extending the area that can be affected by uplift pressure. Large uplift pressures and/or large voids can lead to explosive and catastrophic slab failures, followed by rapid erosion of underlying material. Many spillways and chutes are constructed on soil foundations, making this a widespread issue for the Bureau of Reclamation (Reclamation) and other water resources agencies.

Hydraulic jacking caused dramatic and catastrophic spillway chute failures at Oroville Dam in 2017 and on the fifth drop structure of the St. Mary Canal on the Milk River Project (Montana) in 2020. Further back in Reclamation's history, hydraulic jacking was also responsible for a 1983 failure at Big Sandy Dam and a failure at Dickinson Dam in the 1960s. Void development beneath spillways is a frequent issue on Reclamation projects and hydraulic jacking failure modes are commonly considered in Reclamation risk analysis studies. Recent examples of detected voids include the spillway chutes at Hyrum Dam and Vallecito Dam.

Hydraulic jacking may also occur in channels used for sediment bypass operations, which are lined with granite, basalt, or high-strength concrete panels to resist abrasion. Uplift may also play a role in the failure of tunnel and pipe linings provided for corrosion resistance and friction reduction.

Previous Research

A review of literature and previous Reclamation research on this topic was performed in fiscal year (FY) 2018 as a small scoping project. This included a review of the report of the Independent Forensic Team (IFT) for the Oroville Dam spillway failure, and also a review of two previous Reclamation research studies. Surprisingly, these two studies are the only significant previous laboratory investigations of the problem. The literature review found that previous studies had not yet provided the answers to fundamental questions needed to predict uplift pressures and flow rates through open offset joints subjected to high-velocity flow. The previous studies were performed in test facilities that did not reproduce the boundary layer conditions that are likely to occur in a prototype spillway, and the boundary layer conditions within the test facilities were not measured. As a result, these studies demonstrated relations between uplift pressures and the average channel

velocity, but a potential reduction of uplift pressures due to boundary layer effects suggested by the Oroville Dam IFT report had not been demonstrated experimentally.

Another significant deficiency of the previous studies was limited analysis of test results in a nondimensional manner. Analysis of dimensionless test data (normalized by a reference length or velocity so that results at different scales can be considered as a single data set) is often able to demonstrate important relationships that are obscured in dimensional data.

Objectives

The first objective of the project was to reanalyze data from the previous studies to attempt to address the issues outlined above. Johnson (1976) and Frizell (2007) studied two different flow situations, an open channel operating at atmospheric pressure with relatively low velocities (less than 4.5 m/s) and a pressurized water tunnel with velocities up to 14.6 m/s, respectively. Neither study measured the boundary layer velocity profiles. The 1976 study considered only a sealed foundation, while the 2007 study considered sealed and partially drained foundations and attempted unsuccessfully to measure flow into the foundation.

In an initial effort to test the ideas suggested in the Oroville forensic report, both data sets were combined and adjustments were made to reconcile them with one another, accounting for effects of the water tunnel flow situation that were different from the open channel case. Boundary layer properties were estimated from knowledge of the documented dimensions of the test facilities and relations between uplift pressure and boundary layer velocity were developed. These relations were compared to similar relations developed between uplift pressure and mean (average) channel velocity. Details of this study were published in a peer-reviewed journal article (Wahl et al. 2019) which is provided in Appendix A. An important result was that relations to the mean velocity had less uncertainty than relations to the boundary layer velocity.

The next phase of the study was the design and use of an experimental facility to study two remaining fundamental problems after the completion of the reanalysis of previous data. The objectives of this phase were to:

- Understand the role of boundary layer velocity conditions and develop useful predictive relations for estimating uplift pressure as a function of boundary layer velocities, and
- Develop relationships for estimating flow rate through open offset joints when a partially or fully drained foundation condition exists.

Limitations

Uplift of spillway slabs occurs due to both increased pressure beneath the slab and reduced pressure above the slab in the separation zone that often exists immediately downstream from an offset into the flow. The experimental facility only provided means for measuring the increased pressure below the slab; the pressure reduction on the top surface of the slab is of much smaller magnitude and extent in the flow conditions that produce the most extreme uplift loadings.

The experimental study was limited to the measurement of mean uplift pressures. No attempt was made to measure dynamic pressure fluctuations that occur due to flow turbulence. (Johnson 1976 made dynamic pressure measurements but analyzed them in a relatively limited way.)

Simulated spillway joints in the experimental study were limited to square-edged geometries with joints oriented perpendicular to the flow direction. Frizell (2007) provided some limited data on joints with chamfered and rounded edges.

Experimental Facility & Methods

The facility constructed for this work is a 0.61-m (2-ft) wide flume on a 15° slope, with a jet box provided at the upstream end to regulate the incoming Froude number of the flow, and an adjustable-geometry open joint located about 12.2 m (40 ft) downstream from the jet box, spanning 0.57 m (94%) of the flume width. A sealed chamber equipped with three large 50-mm (2-in.) diameter valves and one smaller air-vent valve is located below the simulated spillway joint. Pressure taps in this chamber are used to measure the uplift pressure generated below the joint in a sealed condition (outlet valves closed) and in various partially vented conditions (one or more valves opened). Flow through the joints is measured through a 90° V-notch weir. In most cases the chamber remains pressurized above atmospheric pressure, so the air-vent valve also discharges water when opened.

The flow conditions above the joint are measured using a 1.32-mm (0.052-inch) diameter Pitot tube that allows the velocity to be determined at any point above the floor of the flume, just upstream from the simulated joint. Velocity profiles are measured for each test condition to define the boundary layer properties near the joint and to obtain an estimate of the flow depth. This estimate is made by fitting a power curve function to the velocity data. This function also allows indirect calculation of the effective flow depth, which is also checked against a depth estimate obtained from a down-looking acoustic sensor. Testing can be performed with mean velocities ranging from 3.5 to 8.8 m/s (11.5 to 29 ft/s). Channel Reynolds numbers range from about 3.4×10^5 to 5.4×10^6 , which should be sufficient to make results independent of friction-related scale effects. Flow conditions for the testing performed thus far have been non-aerated to slightly aerated. Measurements of air concentration have not been made at this time. Figures 1 through 5 show several views of the test facility. Figure 6 shows the joint configuration and the important joint dimensions. Tested gap widths, s , varied from 2.49 to 37.6 mm and offset heights, b , varied from 3.45 to 22.4 mm. The thickness of the joint in the direction normal to the chute slope was 156 mm for all tests before the flow entered the larger 75-mm wide chamber beneath the joint.

All testing was performed with a smooth acrylic floor. Although prototype spillways will almost certainly be somewhat rougher, the objective was not to model a particular surface roughness. Instead, the objective was to measure the actual velocity profile and relate the observed uplift pressures to the true velocities. Relations developed for this purpose should be useful for prototype situations across a range of surface roughness characteristics, if the actual surface roughness can be used to estimate the boundary layer velocity profile.



Figure 1. — Spillway uplift research flume.



Figure 2. — A jet box regulates the depth and velocity of incoming flow.



Figure 3. — Flow attached to the flume floor as it flows over a small-height offset (left); Flow launched or detached from the floor by a large-height offset (right).



Figure 4. — Pitot tube used to measure spillway chute velocity profile.



Figure 5. — Flow exiting the flume through the simulated joint during testing of a partially vented condition. Several valves regulate the back-pressure and control the flow out of the chamber below the joint.

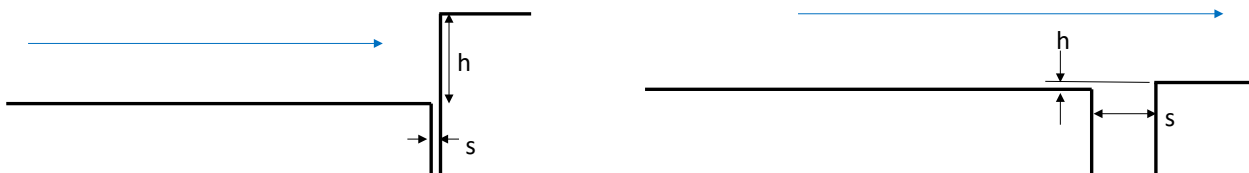


Figure 6. — Simulated spillway joint geometries for small (left) and large (right) β values.

Experimental Results

Due to choppiness of the water surface and limits on the maximum pressure than can be read on the installed manometer boards, velocity profiles could not ever be measured all the way to the water surface. However, Figure 7 shows that there is remarkable consistency of the profiles. These form the basis for most of the ensuing analysis of measured uplift pressures and flow rates.

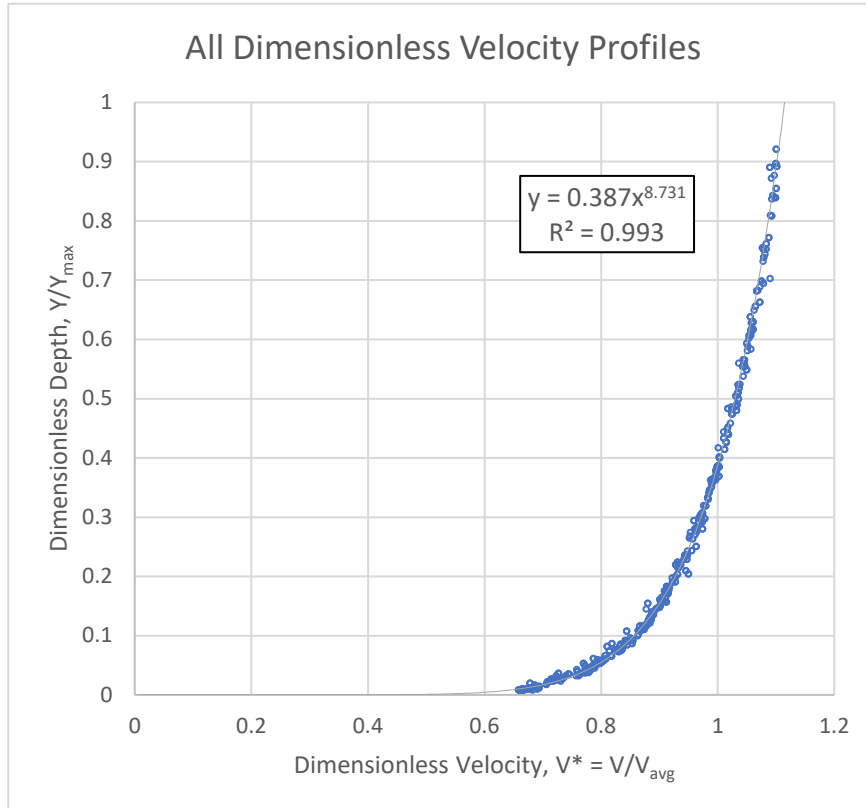


Figure 7. — Dimensionless flow velocity vs. dimensionless depth (aggregated data from all tests).

Uplift Pressures

An early observation was made that the uplift pressure is consistently larger when the flow launches from the offset and detaches from the flume floor. The attached flow condition would be expected in real-world situations during periods of maximum discharge when depths and velocities are large and uplift pressures are the greatest, so this is the condition of greatest research interest. However, for most of the tests both an attached and detached flow condition could be created and sustained, and data were collected for both flow situations. For a few extreme cases only an attached or detached flow condition could be tested.

A first look at the uplift pressure data was made to attempt to validate the relations developed by Wahl et al. (2019). Relating the uplift pressure to the velocity at the mid-height of the offset did not work well (Figure 8). A better fit was obtained when the velocity reference was set near the quarter

point of the offset (25% of the offset height above the floor of the approach channel), but the results were still more scattered than those obtained from relations to the mean channel velocity. Two scenarios are not plotted on Figure 8: a zero offset with a 75-mm wide gap ($\beta = \infty$) and a negative offset of 3.2 mm with a 56-mm gap ($\beta = -17.5$). The first case produced about 3% uplift, and the latter produced very slight suction (negative uplift).

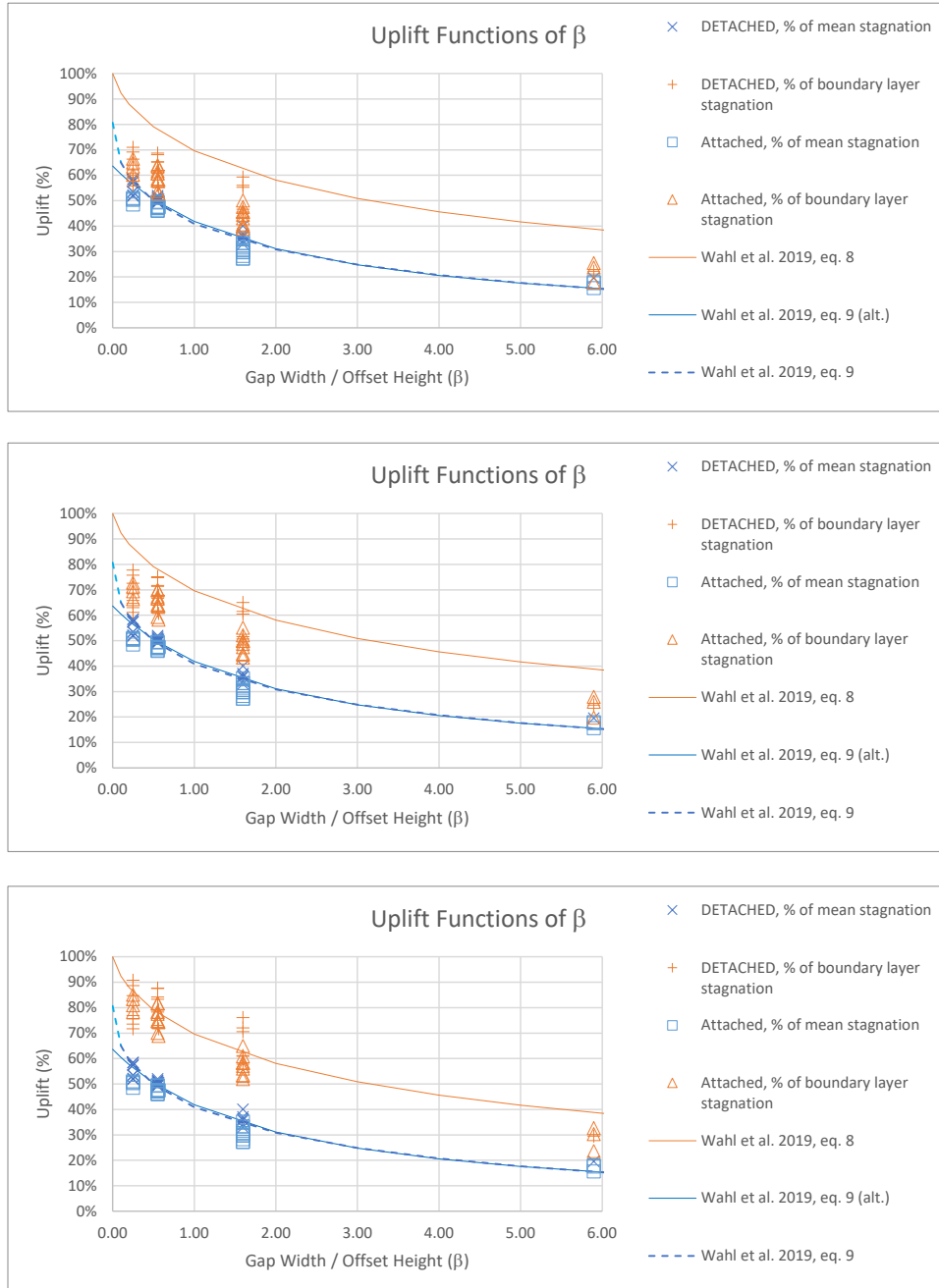


Figure 8. — Relations between observed uplift pressure ratios and the β ratio of simulated offsets. Boundary layer reference velocities are at 75% of the offset height (top), 50% of the offset height (middle), and 25% of the offset height (bottom).

After some consideration of these results, it was concluded that the uplift pressure in different flow conditions is not related well to a boundary layer velocity located at a single fixed fraction of the offset height. Instead, the boundary layer velocity driving the generation of uplift pressure seems located at a varying distance from the floor of the flume. This distance was calculated for each test run and is reported as the stagnation height, y_{stag} . Exploration of many possible relations led to the curve shown in Figure 9 which shows that the stagnation height normalized to the flow depth varies approximately as a power curve function of the quantity $(Fr^*_V)\beta$, where Fr^*_V is a form of roughness Froude number defined as

$$Fr^*_V = \frac{V}{\sqrt{gh}} = \frac{q/y}{\sqrt{gh}}$$

where V is the mean flow velocity, g is the acceleration due to gravity, h is the offset height, q is the discharge per unit width of channel, and y is the flow depth. This unusual Froude number effectively uses two different length references, y and h , and the symbology combines the use of * to indicate that the parameter is dependent on the roughness height and a subscript V to indicate that it is also related to the flow velocity $V=q/y$. This contrasts with the traditional roughness Froude number (usually designated F^* or Fr^*) which uses only the h length reference and is thus independent of the flow velocity. (An investigation was undertaken during this project of the roughness Froude number, which is commonly used in stepped spillway applications and boundary layer flows. That work was submitted as a forum article to the IAHR *Journal of Hydraulic Research*. The paper is currently under review as noted in Appendix B.)

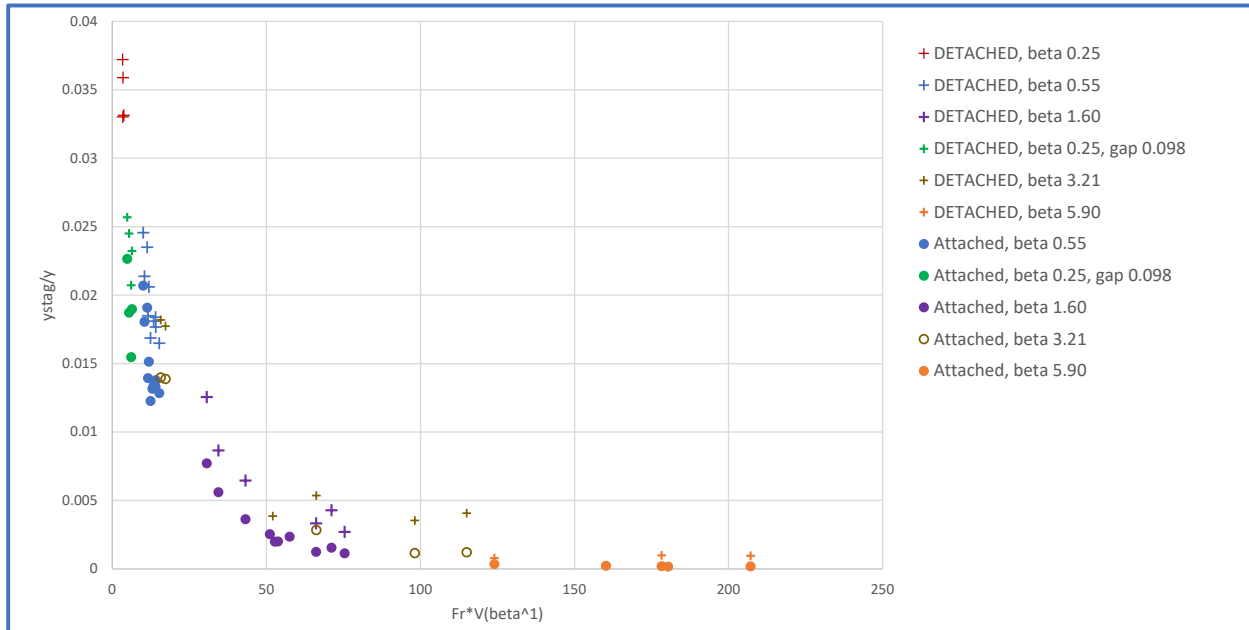


Figure 9. — Approximate power curve relation for the normalized stagnation streamline height.

Other potential relations that might explain the variation of the normalized stagnation height were explored. The relation shown in Figure 9 was judged the most likely to be useful because it most effectively predicted the variation of a set of specific “paired” tests of nearly identical flow rates with significantly different Froude numbers entering the flume (obtained by regulating the inflow with the jet box). Here, the Froude number referred to is the traditional $Fr=V/(gy)^{0.5}$. These paired results are shown in Figure 10. A variation of Figure 9 plotted with log-log scales is shown in

Figure 11. It indicates that the relation in Figure 9 is not a pure power curve, since it is not linear on log-log scales. Modified relations to fully match the shape of this curve are still being explored.

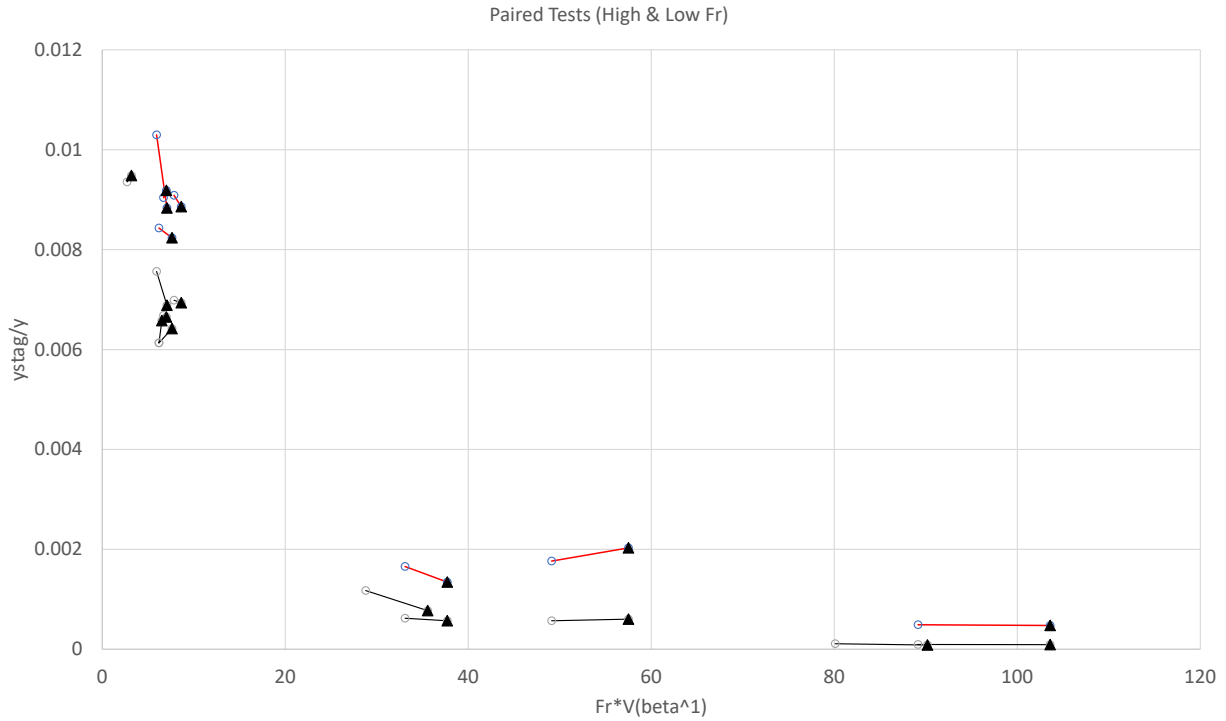


Figure 10. — Uplift pressure relations for paired high- and low-Froude number tests. The trend is similar to Figure 7 for changing values of the independent variable, $(Fr^*V)\beta$.

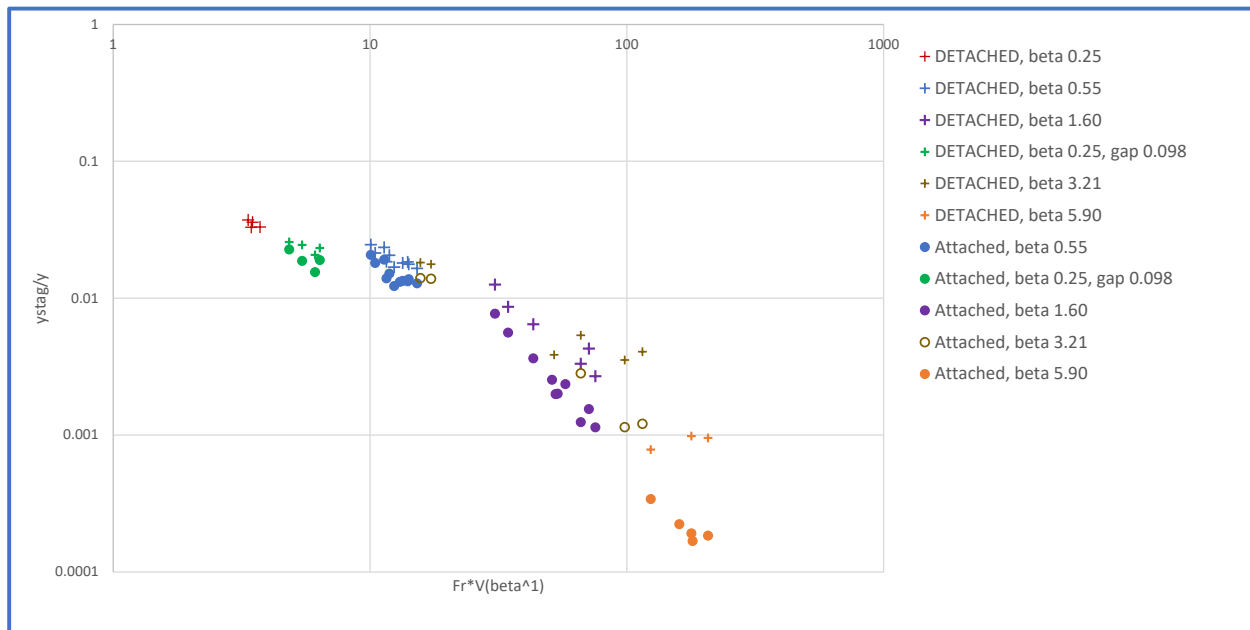


Figure 11. — Normalized stagnation height vs. $(Fr^*V)\beta$.

Flow Rates Through Joints

Flow through the simulated spillway joint was measured for most test conditions using a partially-contracted V-notch weir; flow rate data was not collected for some tests once adequate data had been obtained for each configuration, or when it was not logistically feasible to do so. For each test case, the uplift pressure for the sealed-chamber condition (zero flow through the joint) was noted, and uplift pressures for partially vented conditions were also measured while the flow rate was recorded. The head available to drive flow through the joint was then calculated as the difference between the maximum uplift measured in the sealed chamber and the reduced uplift when the chamber was partially vented. This head was used to calculate the discharge coefficient for an orifice equation applied to the open joint.

Figure 12 shows the resulting relationship for tests with large and small values of β = gap width / offset height, with the discharge coefficient varying as a function of the ratio of flow velocity through the gap to mean velocity over the joint. A preliminary equation for the curve shown on the figure is $C_d = 1 / [0.051(V_{\text{gap}}/V_{\text{channel}})^{-1.1} + 1]$. Data will continue to be collected in a follow-up project and this equation may be refined. The application of this equation seems challenging at first, since the velocity ratio is unknown until the discharge coefficient and flow rate has been determined. However, the problem can be solved readily by assuming an initial discharge coefficient (e.g., 0.8) and calculating the flow rate and velocity ratio. The assumed discharge coefficient can then be adjusted and the procedure repeated. Convergence of the solution occurs quickly.

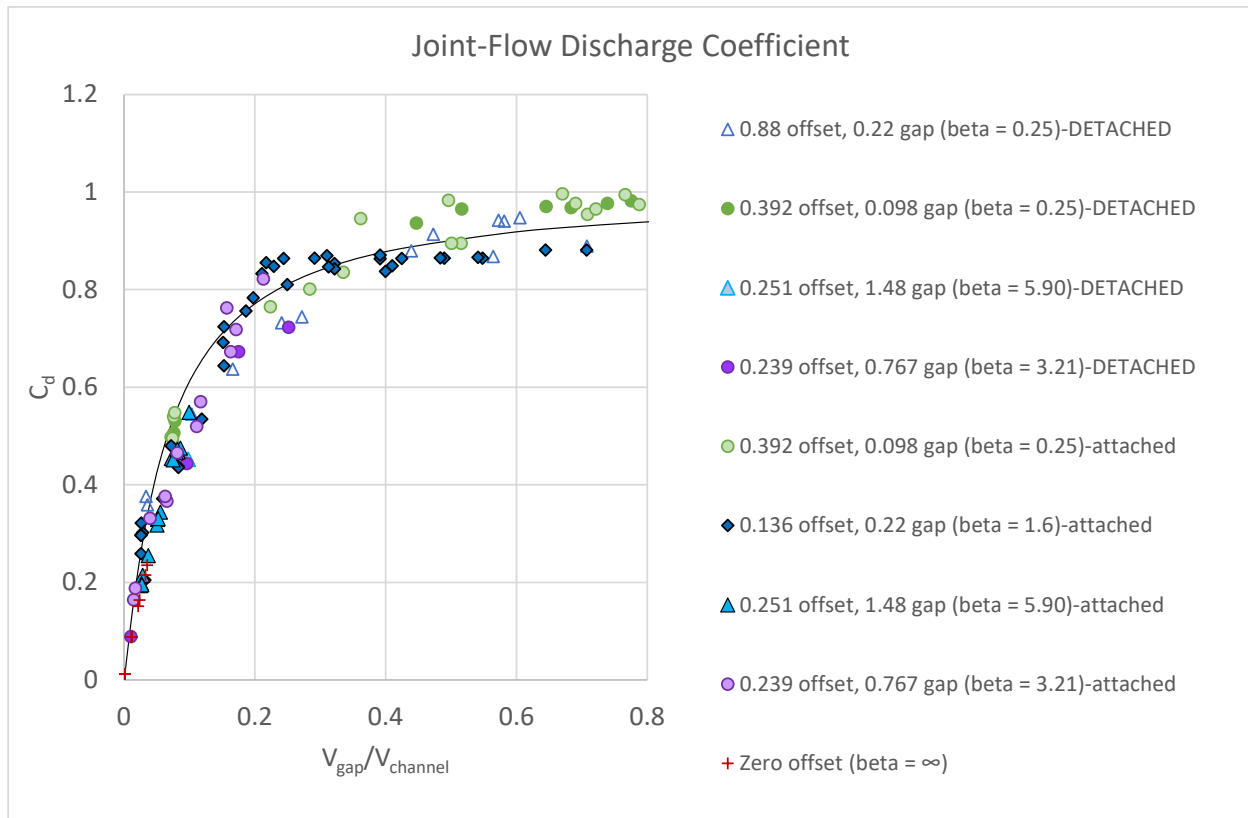


Figure 12. — Curve relating observed joint flow discharge coefficients to the velocity ratio at the joint entrance.

A small number of data sets exhibited a much different and more scattered behavior shown in Figure 13. Initially this was believed to be due to an anomaly of the test apparatus, but further investigation is confirming that it is a real behavior with high variability. The best working theory at this time is that it is caused by a separated flow zone at the entrance to the gap which only occurs for a small range of β ratios. Additional work is needed to understand the flow conditions that create this unusual behavior.

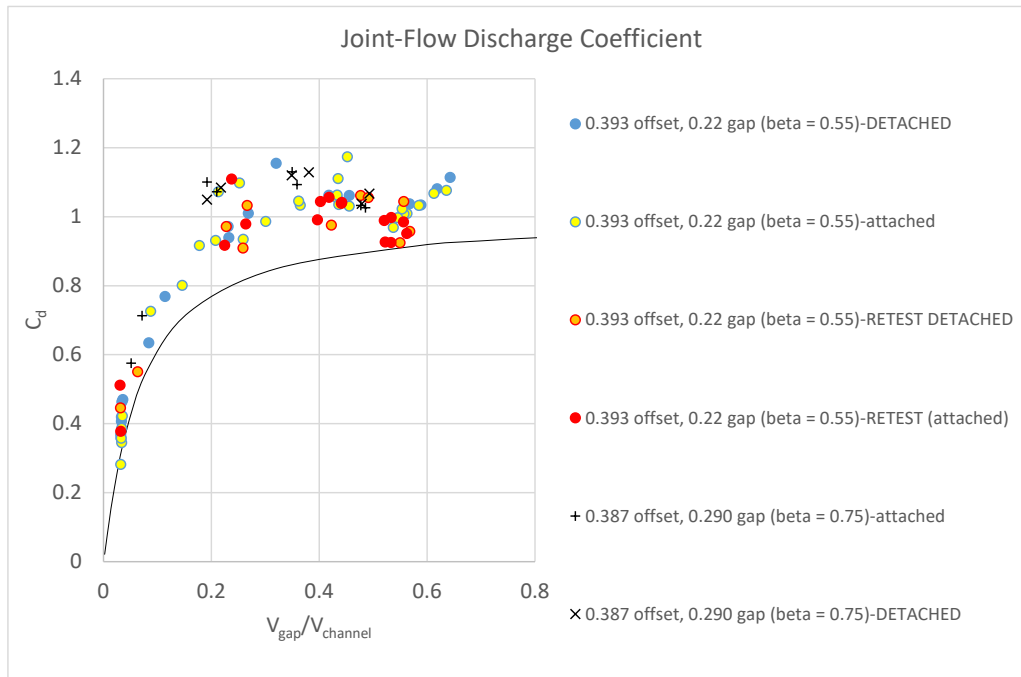


Figure 13. — Different and inconsistent relation between the discharge coefficient and the gap-to-channel velocity ratio for $\beta=0.55$ and $\beta=0.75$.

Separately Published End Products

- A paper was published in 2019 in the *Journal of Hydraulic Engineering* (American Society of Civil Engineers, ASCE). This article summarizes the investigation and reanalysis of previous laboratory test data located during the literature review phase of the project.
- A forum article was submitted in 2021 to the *Journal of Hydraulic Research* (International Association for Hydro-Environment Engineering and Research, IAHR). This article discusses the history and physical significance of the roughness Froude number, a parameter that is important in the study of stepped spillways and boundary layer flows. A variation of the roughness Froude number was related in this project to the location of the stagnation streamline that drives the uplift pressure generated within an open offset spillway joint.
- A future paper will be submitted to either the ASCE *Journal of Hydraulic Engineering* or the IAHR *Journal of Hydraulic Research* with the results of the laboratory testing performed in 2021, as summarized in the Experimental Results section above.

Project Data

Experimental data related to this project are maintained on Reclamation's computer network at the Technical Service Center. This is an active research area with continuing work. Data will continue to be added to this site.

Project Folder: \\bor\do\TSC\Jobs\DO_NonFeature\Science and Technology\2018-PRG-Spillway Chute Joints

Contact Person: Tony Wahl

Quantity of Files: 1.2 GB (as of September 30, 2021)

Data Types: Spreadsheets, documents, photographs, video, Powerpoint presentations.

References

Frizell, K.W., 2007. *Uplift and Crack Flow Resulting from High Velocity Discharges over Open Offset Joints*. Report DSO-07-07, Bureau of Reclamation Dam Safety Technology Development Program, Denver, CO. https://www.usbr.gov/tsc/techreferences/hydraulics_lab/pubs/DSO/DSO-07-07.pdf

Hepler, T.E., and P.L. Johnson, 1988. Analysis of spillway failures by uplift pressure. In: *Hydraulic Engineering*, Proceedings of the 1988 National Conference on Hydraulic Engineering and International Symposium on Model-Prototype Correlations, ASCE, Colorado Springs, Colorado, Aug. 8-12, 1988. S.R. Abt and J. Gessler, editors. <http://cedb.asce.org/CEDBsearch/record.jsp?dockey=0057459>

IFT, 2018. *Independent Forensic Team Report: Oroville Dam Spillway Incident*, January 5, 2018. [https://damsafety.org/sites/default/files/files/Independent Forensic Team Report Final 01-05-18.pdf](https://damsafety.org/sites/default/files/files/Independent%20Forensic%20Team%20Report%20Final%2001-05-18.pdf)

Johnson, P.L., 1976. Research into uplift on steep chute lateral linings. Memorandum to the Open and Closed Conduit Systems Committee, Bureau of Reclamation, Denver CO. https://www.usbr.gov/tsc/techreferences/hydraulics_lab/pubs/PAP/PAP-1163.pdf

Schwalt, M. & W.H. Hager, 1992. Die Strahlbox (The jetbox). *Schweizer Ingenieur und Architekt* 110(27-28): 547-549 (in German). <https://doi.org/10.5169/seals-77937>

Trojanowski, J., 2004. Assessing failure potential of spillways on soil foundation. Association of State Dam Safety Officials Annual Conference, Lexington, KY.

Trojanowski, J., 2008. DAM SAFETY: Evaluating Spillway Condition, *Hydro Review*, Vol. 27, Issue 2, April 2008. <https://www.hydroworld.com/articles/hr/print/volume-27/issue-2/technical-articles/dam-safety-evaluating-spillway-condition.html>

Wahl, Tony L., K. Warren Frizell, and Henry T. Falvey, 2019. Uplift pressures below spillway chute slabs at unvented open offset joints. *Journal of Hydraulic Engineering*, 145(11): 04019039. [https://doi.org/10.1061/\(ASCE\)HY.1943-7900.0001637](https://doi.org/10.1061/(ASCE)HY.1943-7900.0001637)

Appendix A

This appendix contains a non-copyrighted, pre-print version of:

Wahl, Tony L., K. Warren Frizell, and Henry T. Falvey, 2019. Uplift pressures below spillway chute slabs at unvented open offset joints. *Journal of Hydraulic Engineering*, 145(11): 04019039.
[https://doi.org/10.1061/\(ASCE\)HY.1943-7900.0001637](https://doi.org/10.1061/(ASCE)HY.1943-7900.0001637)

HY11491

Uplift Pressures Below Spillway Chute Slabs at Unvented Open Offset Joints

Tony L. Wahl, Member, P.E.¹; K. Warren Frizell²;
and Henry T. Falvey, Life Member, Dr.Ing., Hon. D.WRE³

Abstract

The catastrophic failure of the spillway chute at Oroville Dam in February 2017 raised concerns throughout the water resources industry regarding design, construction and maintenance practices for concrete spillway chutes, especially joints and cracks that could allow penetration of high pressure water into a chute foundation. The independent forensic team investigation found that hydraulic jacking was the most likely cause of the initial chute slab failure, highlighting a need for better analysis of the hydraulic jacking potential of existing spillways and more resilient designs for spillways that operate under high-velocity flow conditions. This paper reviews the Oroville Dam event and findings and previous laboratory testing performed to evaluate uplift pressures and flow transmitted through spillway joints. A reanalysis of previous studies was used to develop relations between chute velocity, joint geometry, and uplift pressure transmitted into a joint. Uplift pressure head in these relations is expressed in a dimensionless manner, either as a percentage of the velocity head in the boundary layer at the mid-height of the offset into the flow, or as a percentage of the channel-average velocity head. The first approach is potentially more useful for prototype applications, but the second method provides the best fit to the available experimental data. Additional research is still needed to quantify rates of flow through open joints, confirm relations between uplift pressure and boundary layer velocities, and evaluate the effects of aerated flow.

Introduction

The February 2017 failure of the spillway chute at Oroville Dam, owned and operated by the California Department of Water Resources (DWR), raises significant concerns about aging spillway structures. As dams and spillways age, concrete surfaces and masses slowly deteriorate, slabs may shift due to foundation settlement or frost heave, reinforcement bars and anchors may

¹ Technical Specialist, Bureau of Reclamation, Hydraulic Investigations and Laboratory Services, Denver, CO 80225-0007.

² Retired; formerly, Hydraulic Engineer, Bureau of Reclamation, Hydraulic Investigations and Laboratory Services, Denver, CO 80225-0007.

³ Consultant, Henry T. Falvey & Associates, 11624 Blackfoot Rd., Conifer, CO 80433.

corrode and lose strength, and auxiliary components such as under-slab drain systems can be compromised by sediment deposition, scour, and intrusion of tree roots. Once concrete surfaces suffer initial deterioration, other problems become more likely, including cavitation damage, increased uplift forces at joints, and acceleration of deterioration rates due to freeze-thaw action.

One of the most likely locations for problems to occur in a concrete spillway chute is at or near the joints. Common types of joints include construction joints, control joints, expansion joints, and contraction joints. Joints typically deteriorate faster than slabs, and joints offer opportunities for surface offsets and entry of pressurized flow into foundation areas, key elements for cavitation and hydraulic jacking failure modes. Even if uplift pressures are not large enough to cause immediate slab movement, the flows that enter the foundation through open joints can cause erosion and the development of voids beneath slabs that may ultimately lead to slab movement, offsetting of joints, and uplift. Despite these problems, joints are a practical necessity since spillways are large structures that typically must be constructed in a specific sequence and in multiple phases over several months or years. Joints placed at regular intervals enable staged construction, permit thermal contraction and expansion, and help to control cracks in the finished product. The geometry and construction details of joints vary, which affects their vulnerability to uplift and seepage flow. Although modern design standards for spillway joints (e.g., Bureau of Reclamation 2014) include details meant to prevent the development of offsets and gaps (e.g., keys and structural reinforcement) and limit flow through joints (waterstops), older spillways like Oroville lack some or all of these features or have other deficiencies (e.g., poorly prepared foundations, inadequate or deteriorated drainage systems, etc.) that make them vulnerable to uplift failures.

Hydraulic jacking occurs when the forces acting to lift a spillway slab exceed the forces resisting upward movement. Resisting forces include the weight of the slab itself, the capacity of foundation anchors, and the pressure applied to the top of the slab by water flowing in the chute. Uplift can be created through a combination of increased pressure below the slab and reduced pressure above the slab (i.e., lift). High pressures can be generated below a slab when high-velocity flow stagnates against an offset into the flow at a joint that is open to the foundation. Offsets can occur due to settlement of an upstream slab or lifting or tilting of the edge of a downstream slab, or with no slab movement when the concrete surface is spalled upstream from a joint. Slab movements that lead to offsets may occur due to drying or wetting of soil foundations, frost heave, or as a result of internal erosion of foundation soils when flow through open joints is not captured or retained within a drainage system. When internal erosion leads to the development of large voids beneath a slab, this may enable high pressures generated at a joint to more readily act over a large area beneath the slab.

Lift on the top surface of a slab can occur due to gradual curvature of the spillway surface away from the flow, or abrupt separations of flow from the spillway surface. Steps up or down caused by misalignment of joints are both capable of generating localized low pressure zones. Dong et al. (2010) studied cavitation at offsets into the flow and measured negative pressures approaching the vapor pressure of water in the separation zone downstream from 2- and 5-mm-high offsets, but pressure recovery was also observed to begin within 75 to 100 mm downstream. Vapor pressure establishes the minimum possible pressure on the upper surface of a spillway slab, limiting the contribution of flow separation to uplift head to about 10 m (33 ft), but stagnation pressure heads associated with high-velocity flow can be much larger. For example,

the stagnation pressure associated with a velocity of 30 m/s (98 ft/s) is about 46 m (151 ft). For this reason, most analyses of uplift forces have focused on the pressure increase beneath the slab. In previous experimental work to be discussed later in this paper, the reported uplift is the net difference between the increased pressure below the slab and the pressure above the slab associated with a relatively shallow flow depth.

Additional factors that may be important in spillway slab uplift are air entrained in the flow above the slab and its effect on pressures generated within the joints, and the role of fluctuating pressures in combination with steady uplift. These two factors may also be linked to some degree, as Bollaert and Schleiss (2003a, 2003b) have shown that air is an important factor in creating a resonance effect that magnifies pressure fluctuations within closed end fissures in fractured rock masses.

Hepler and Johnson (1988) and Trojanowski (2004) documented hydraulic jacking failures in Bureau of Reclamation spillways at Dickinson Dam (North Dakota) in 1954 and at Big Sandy Dam (Wyoming) in 1983. At Dickinson Dam there was a lack of defensive design features such as foundation grouting, anchor bars, and waterstops, and the underdrain system was compromised by subfreezing temperatures. In addition, there were several possible mechanisms that could have led to joints with offsets and openings that permitted pressurized flow to enter the foundation. Unfiltered gravel zones around the underdrain system were also implicated as a factor in internal erosion that led to the development of voids beneath the slabs. At Big Sandy Dam, freezing temperatures over many years caused deterioration of the spillway concrete, damage to the underdrain system, and slab movement that produced open and offset joints. Uplift pressures at the time of failure were large enough to pull the foundation rock anchors out of the soft sandstone foundation (1.2-m [4-ft] long, 25-mm [1-inch] diameter bars on 1.5-m [5-ft] centers, with a design capacity of 44 kN [10 kips] each). It was speculated that the anchors may have been only 50 percent effective due to deterioration of the grout-foundation contact and could have been failed by an uplift pressure head greater than 49 percent of the mean velocity head, which was a feasible failure scenario (Trojanowski 2004). Considering these failures and experiences from other spillways exhibiting various types of distress, Trojanowski (2008) discussed the evaluation of potential failure modes of spillways, including factors related to hydraulic jacking.

The Oroville Dam Spillway Failure

The description of the Oroville Dam spillway chute failure incident given in this section is summarized from the report of the Oroville Dam Independent Forensic Team (IFT 2018).

Oroville Dam is an embankment dam located on the Feather River in northern California—the tallest dam in the United States at 235 m (770 ft). The dam is owned and operated by DWR, which was responsible for design and construction, completed in 1968. The dam is one component of the Oroville-Thermalito Complex, which includes several hydroelectric powerplants, canals, and diversion and fish barrier dams. The complex is a major feature of the California State Water Project, the largest state-owned water storage and delivery system in the United States. On February 7, 2017 the service spillway chute lining failed, leading to an emergency that lasted for several weeks while the spillway was required to continue operating.

At the time of the failure Oroville Dam was equipped with two spillways. The gated spillway, described as the service spillway or Flood Control Outlet (FCO), was controlled by eight large top-seal radial gates and discharged into a concrete chute that was 54.5 m (178.67 ft) wide and 914 m (3000 ft) long. The emergency spillway, which had never operated, was a 518-m (1700-ft)-long uncontrolled overflow weir discharging into an unimproved steep natural drainage leading back to the Feather River. The service spillway chute was originally designed for a maximum flow rate of 7080 m³/s (250,000 ft³/s). The historical maximum instantaneous discharge was 4530 m³/s (160,000 ft³/s) in 1997, about 64% of the design discharge (IFT 2018). The spillway had operated infrequently in its 49 year history, with about 4 days of operation above 2830 m³/s (100,000 ft³/s), 40 days above 2120 m³/s (60,000 ft³/s), and 300 days above 1060 m³/s (30,000 ft³/s). Soon after construction was completed, cracking of the spillway slab occurred over embedded drain pipes, which were arranged in a herringbone pattern down the length of the spillway. As result, there was a long history of periodic repairs made to maintain the service spillway chute slab.

Due to heavy snow and rain in northern California in the winter of 2016-2017, the service spillway operated for about 5 days in mid-January 2017 at flow rates up to about 283 m³/s (10,000 ft³/s), the first significant flows since 2011. The spillway was shut down around January 20 and then restarted around February 1. Discharges were gradually increased during early February. At about 10:10 a.m. on the morning of February 7, while the discharge was being increased from 1200 to 1490 m³/s (42,500 ft³/s to 52,500 ft³/s), DWR personnel working near the left side of the service spillway chute heard a loud sound they compared to an explosion. They subsequently observed spray and significantly disturbed flow conditions in the spillway chute near station 1020 m (33+50 ft), about 640 m (2100 ft) downstream from the spillway radial gates. The spillway continued to operate for about one hour, and then from about 11:25 a.m. to 12:25 p.m. the spillway gates were closed, revealing the damage shown in Figure 1.

Due to forecasted large inflows, a continued need for spillway operations was anticipated. Following initial damage assessments and release of some closely monitored test flows, the spillway was placed back into service from Feb. 8-10 at discharges up to 1840 m³/s (65,000 ft³/s), with erosion and damage to the chute structure continuing. Unfortunately, these releases were not enough to keep up with inflow to the reservoir. Early on February 11 the reservoir level exceeded elev. 274.62 m (901 ft) and the emergency spillway began to flow for the first time in its history. The reservoir level eventually reached elev. 275.11 m (902.59 ft) at about 3:00 a.m. on February 12, with a peak flow of about 354 m³/s (12,500 ft³/s) over the emergency spillway crest. There was extensive erosion and headcutting in the natural channel below the emergency spillway crest, and headcuts advancing upstream toward the spillway crest threatened its stability. At 3:35 p.m. on February 12 the service spillway gate openings were increased to draw the reservoir down and reduce flows over the emergency spillway crest. At 3:44 pm on February 12, an evacuation order was issued for about 188,000 downstream residents due to the rapidly progressing erosion in the emergency spillway discharge channel. The service spillway flows reached 2830 m³/s (100,000 ft³/s) by about 7:00 p.m. on February 12 and were maintained there for about 3.5 days through 8:00 a.m. on February 16. During this period the reservoir levels dropped significantly and the situation stabilized. Service spillway flows were gradually reduced over subsequent days until the spillway was shut down again on February 27. After new inspections, the service spillway was placed back into operation in early March and operations

continued until it was shut down for the season on May 19. The damage to the spillway at the end of the operating season is shown in Figure 2.

Forensic Investigation

A six-member Independent Forensic Team (IFT) (including the third author) was formed after the Oroville Dam spillway slab failure, with the following charge:

“To complete a thorough review of available information to develop findings and opinions on the chain of conditions, actions, and inactions that caused the damage to the service spillway and emergency spillway, and why opportunities for intervention in the chain of conditions, actions, or inactions may not have been realized.

Their report issued in January 2018 provides the IFT’s opinion on the physics of the failure process and the most likely failure modes. The report also identifies physical factors and features of the design that contributed to the failure and identifies organizational and human factors that contributed to the failure and affected the response to the emergency.

The IFT concluded that the spillway chute failure most likely was initiated by uplift and removal (hydraulic jacking) of a section of the chute slab near Sta. 1020 m (33+50 ft), just downstream from the end of the vertical curve in the chute that transitions from a 5.67% slope to a 24.5% slope. High-velocity flow then rapidly eroded moderately to highly weathered rock and soil-like foundation materials beneath adjacent slabs. The initial uplift failure was believed to have affected only part of one of the 12.2- by 15.2-m (40- by 50-ft) chute slab panels, and could have removed something as small as a localized repair patch or a spall above a drain, or as large as a 6-m (20-ft) section located between cracks that existed above the herringbone drains partially embedded in the bottom of the slab. Once the initial portion of the slab failed, it probably triggered a rapid chain of subsequent events, leading to additional slab section failures (IFT 2018).

The IFT report discussed the possibility of an initial failure due to sagging or settling of a slab into a void beneath the slab. The team could not absolutely rule out this possibility, but found it less likely than an uplift failure for several reasons, including the suddenness of the failure, eyewitness reports of explosion-like sounds, and a lack of any evidence of sagging in photos taken of the spillway after the operations in early January 2017. The team also allowed for the possibility that localized settlement upstream from a joint or crack could have created an offset into the flow that led to injection of high pressure water beneath the slab downstream from that location.

Contributing Factors

Several physical factors were cited by the IFT that contributed to the initial failure and subsequent damage to the spillway chute. Although the team was confident that the initial failure occurred due to uplift created by high-velocity flow being injected through a feature of some kind in the chute slab surface, they could not pinpoint the specific type or exact location of the feature. Possibilities they listed included: open joints, unsealed cracks over lateral drainage pipes (the herringbone drains), spalled concrete at either a joint or drain location in a new or previously repaired area, or some combination of multiple features. The IFT made calculations of potential discharges through cracks and joints and believed that the flows could have far

exceeded the localized capacity of the drain system, causing flow to back up in the drains and increase uplift forces.

Several contributing factors were specifically listed by the IFT as possible explanations for why the spillway chute failed in 2017 at a discharge of about 1490 m³/s (52,500 ft³/s), but had not failed in earlier high-flow events, such as a release of more than 1980 m³/s (70,000 ft³/s) in 2006 and the maximum discharge of 4530 m³/s (160,000 ft³/s) in 1997. All of these contributing factors are related to slow changes in the condition of the spillway materials or foundation over time.

- New chute slab damage and/or deterioration of previous slab repairs,
- Expansion of relatively shallow void(s) under the slab, through erosion or shrinkage of clay soils,
- Corrosion of steel reinforcing bars or dowels across the concrete cracks or joints, and
- Reduction in anchor capacity

Hydraulic Analyses

Appendix B of the IFT's report provided detailed analysis and discussion of hydraulic phenomena that were considered by the team in connection with their efforts to identify the initiating cause of failure and contributing factors.

Stagnation and Uplift Pressures

To evaluate the potential uplift pressures that could act on a spillway slab, the IFT report described an approach to estimating the stagnation pressure that could occur at a vertical offset into the flow. When flow strikes the face of such an offset, flow is deflected downward into the joint and up and over the offset. At the dividing line between these flows, the flow stagnates against the face of the offset and the kinetic energy of the flow is converted into potential energy in the form of pressure head—the *stagnation pressure*. With an opening in the joint, all or a portion of the stagnation pressure can be transmitted through the joint, creating uplift beneath the slab. The stagnation pressure can also drive flow into the joint, and this flow must be carried away by the drainage system beneath the slab to avoid a buildup of pressure.

In a prototype spillway with a long chute, a velocity profile develops in the chute with low velocities near the bed and high velocities near the water surface. The greatest variation of velocities occurs very near the bed in the boundary layer. At a significant distance down the chute, the thickness of the boundary layer could be enough for offsets at spillway joints to be contained entirely within the boundary layer. In this case, flow offsets would be exposed to velocities that are lower than the average velocity within the whole channel. Referring to studies of flow over open offset joints by Frizell (2007) that utilized Particle Image Velocimetry (PIV) to map velocity fields approaching a joint, the IFT report suggested that the streamline of the flow stagnating against the face of an offset into the flow tended to be located at about half of the offset height. With the failure taking place about 640 m (2100 ft) downstream from the control gates, the boundary layer was estimated to have a thickness of about 1 m (3.3 ft), with a well-developed velocity profile in the channel. To estimate the velocity at various heights above the channel floor that might correspond to the mid-height of offsets of different sizes, the IFT used

an equation provided by Rouse (1945, p. 199, Eq. 157) to describe the velocity profile versus depth in an open channel flow:

$$\frac{v_y - V}{V\sqrt{f}} = 2 \log_{10} \frac{y}{y_0} + 0.88 \quad (1)$$

where v_y = velocity at distance y above the boundary
 f = Darcy-Weisbach friction factor
 y = distance from the boundary
 y_0 = total flow depth
 V = mean flow velocity

It is important to note that y_0 is the total flow depth and that Eq. 1 computes an estimate of the entire velocity profile from the boundary to the free surface, not just the velocity within the boundary layer near the bed. (The IFT report incorrectly identified y_0 as the depth where the velocity is zero.) This equation is sensitive to the surface roughness through the friction factor, f , so rougher surfaces will have a more pronounced velocity profile with lower velocities near the channel bed. Once v_y is estimated, the associated stagnation pressure is

$$\frac{P_s}{\gamma} = \frac{v_y^2}{2g} \quad (2)$$

where P_s = stagnation pressure
 γ = unit weight of water
 v_y = approach velocity of the stagnated flow
 g = acceleration due to gravity

Table 1 shows stagnation pressures estimated at 50% of the offset height for two flow rates and three joint offset heights. The two flow rates bracket the conditions at the time of the initial Oroville failure, and the flow depths and velocities at the station of the failure are determined from water surface profile calculations (Falvey 1990; Wahl et al. 2019), assuming a surface roughness of 0.3 mm (0.001 ft). This table is similar to Table 2 in Appendix B of the IFT report, but corrects three problems that affected that table: 1) velocities were calculated at the tip of the offset, even though the text of the IFT report said they were calculated at the mid-height; 2) stagnation pressure head values were actually velocities that had not yet been converted to pressure head; and 3) incorrect friction factors were used that were much too large. In the present Table 1, friction factors were determined with the Colebrook-White equation as an integral part of the water surface profile calculations. In this particular example, the combined corrections for these three problems largely offset one another, so the numerical values of stagnation pressure head in Table 1 are not dramatically different from those given in the IFT report.

The stagnation pressures shown in Table 1 can become the source for generating uplift pressure beneath a slab, but the IFT report emphasized that there is uncertainty regarding the extent over which the uplift force would act. The type of drain system beneath the joint or the porosity and permeability of soils beneath the joint would affect the distribution and extent of uplift pressures. The IFT report did not estimate a probable pressure distribution or total uplift force on a whole

slab or portion of a slab, but used the analysis only to show the magnitude of uplift pressures that could have been generated and the trends for increasing uplift pressure with increasing discharge. The stagnation pressure head increases 22% when the flow rate increases 80% from 850 to 1530 m³/s (30,000 ft³/s to 54,000 ft³/s). Note that the estimated stagnation pressures are small fractions (30% to 50%) of the total velocity head of the mean flow, which illustrates the significant effect of basing the stagnation pressure estimates on the velocity near the surface, rather than on the mean channel velocity. This analysis is sensitive to the assumed hydraulic roughness of the flow surface. With increased roughness the calculated stagnation pressures drop significantly and there is greater sensitivity to the offset height.

The analytical approach taken by the IFT depended on some significant assumptions. For a given joint offset height, the uplift pressure is estimated by assuming that stagnation of the velocity occurs at 50% of the offset height, and that 100% of this stagnation pressure is transmitted through the joint. Each of these assumptions should be verified with either lab or field testing. In addition, to apply this analysis to the practical problem of determining the net uplift force, the drainage system and/or underlying foundation must be analyzed to determine how drainage will dissipate the uplift pressure. Once the resulting uplift forces are estimated, the design of the slab and its anchorage can be evaluated to determine if the slab can withstand the applied loads.

Flow through Joints or Cracks

The IFT report analyzed the potential for seepage or leakage flow through open spillway joints or cracks. The analysis used the energy equation applied to the slot behaving as a pressurized conduit experiencing turbulent flow. The analysis considered only joints and cracks that were flush, with no offset into or away from the flow. The driving force for flow through the joint was only the hydrostatic pressure associated with the spillway flow depth, not any stagnation pressure. No quantitative estimates were made of the density of cracking in the slab or the prevalence of open joints, but the IFT found that the drainage system beneath the Oroville Dam spillway chute would have been unable to convey the volume of flow that might have come from the widespread open joints or cracks.

The analysis performed by the IFT did not consider the increased flow through a joint that could occur due to stagnation pressure developing against the entrance to an offset joint. Laboratory testing has not yet provided reliable information that can be used for this purpose.

Previous Research

Despite the historical cases of spillway chute slab failure by hydraulic jacking, efforts to quantify the uplift pressures generated by high-velocity flows over offset and open spillway joints have been very limited. Most studies of uplift have focused on slabs and joints in stilling basins and plunge pools, where fluctuating pressures generated by hydraulic jumps and impinging jets are the driving mechanism (Toso and Bowers 1988; Fiorotto and Rinaldo 1992a, 1992b; Bellin and Fiorotto 1995; Fiorotto and Salandin 2000; Melo et al. 2006; Liu and Li 2007; Mahzari and Schleiss 2010; González-Betancourt and Posada-García 2016). Bowers and Toso (1988) describe a model study intended to study this mechanism in the failure of one specific spillway stilling basin. Fiorotto and Caroni (2014) and Barjastehmaleki et al. (2016a, 2016b) considered

how the high pressures generated at stilling basin slab joints propagate beneath the slab and dissipate with increasing distance from the joint.

High pressures generated in the joints and cracks of rock masses have also been studied extensively as a driving mechanism for scour in rocky plunge pools and unlined rock channels (Bollaert and Schleiss 2005; Pells 2016), but not with a focus on joints with the regularity or extent of those found in concrete spillway linings. Most of this work has been directed toward the prediction of removal of individual rock blocks or the breakup of large rock masses into smaller units due to intense pressure fluctuations on rock surfaces or within joints. Key features of the flows driving these processes are impingement of jets at angles ranging from normal to acute, aeration and disintegration of jets both above and below the water level of the pool, and sizable pressure fluctuations applied to slab surfaces and joints. These characteristics stand in sharp contrast to gradually varied flows that are essentially parallel to relatively smooth spillway chutes. The flume study by Pells (2016) produced measurements of pressure generated within the joints surrounding an idealized rock block projecting into a high-velocity open-channel flow similar to that in a spillway chute, but included many three-dimensional effects that would be absent or much different for flow over a typical chute slab joint.

To the authors' knowledge, the only studies of uplift pressure due to unidirectional high-velocity flow over offset spillway joints are those of Johnson (1976) and Frizell (2007), both conducted in the Hydraulics Laboratory of the Bureau of Reclamation. Those two studies will be reviewed here and the data further analyzed with a view toward application to situations like the event at Oroville Dam.

Open-Channel Tests

Johnson (1976) studied uplift pressures beneath spillway chute slabs using a 152-mm (6-inch) wide by 2.44-m (8-ft) long open channel flume that contained an open joint with a vertical offset into the flow located 0.91 m (3 ft) from the downstream end. The width of the joint opening (gap) was set to values of 3.2, 6.4, 12.7, and 38.1 mm ($\frac{1}{8}$, $\frac{1}{4}$, $\frac{1}{2}$, and $1\frac{1}{2}$ inches) and the size of the vertical offset was set to 3.2, 6.4, 19.1, and 38.1 mm ($\frac{1}{8}$, $\frac{1}{4}$, $\frac{3}{4}$, and $1\frac{1}{2}$ inches). In photos, the flume appears to be level, but the exact slope is undocumented. Flow was provided through an adjustable vertical slide gate that allowed the flow velocity at the offset to be varied from 2.29 to 4.57 m/s (7.5 to 15 ft/s), as measured by a Pitot tube (presumably positioned upstream from the offset joint). The open joint allowed water to enter a chamber beneath the flume that was tightly sealed. Pressures in this chamber were measured using a dynamic pressure transducer whose output was recorded on a strip-chart. The joints studied were all oriented normal to the bed of the flume and extended perpendicular to the flow direction across the full width of the flume.

Average pressure values and a value that exceeded 95% of the instantaneous dynamic pressures were both determined from the strip-chart records. The latter was arbitrarily selected as a value representative of maximum uplift pressures at a spillway slab. Net uplift pressure heads were reported as the difference between the high pressure in the chamber and the average depth of flow measured over the joint, but separate pressure and depth measurements were not reported. Uplift pressure heads were presented as dimensionless percentages of the computed velocity head corresponding to the average flow velocity in the channel for each test, but the data were

not analyzed using any dimensionless measure of the offset heights and gap widths. Also, although the discussion suggested that uplift pressures should be related to the conditions in the boundary layer and that trends in observed uplift in the experiments were consistent with this idea, no attempt was made to quantitatively relate the uplift pressures to boundary layer velocities instead of the channel-average velocity. Boundary layer characteristics were not measured during the experiments, nor were any attempts made to analytically estimate the boundary layer conditions of the tests.

Notable trends observed in the data were:

- Uplift pressures increased with smaller gap widths. This was attributed to larger gaps allowing larger or stronger flow circulation cells to develop within the gap, dissipating some of the flow energy and reducing the uplift pressure transmitted through the gap. Another explanation is that a larger portion of the gap width was exposed to pressures below the stagnation pressure, since true stagnation of the flow only occurs at the face of the offset.
- Uplift pressures increased for larger vertical offsets, most rapidly when vertical offsets were small. At large vertical offset heights, the uplift pressure tended to approach a constant percentage of the velocity head.
- For higher velocities, the uplift pressures tended to be a slightly smaller percentage of the channel-average velocity head.

Specific flow depths, discharges, and channel slope data for each test were not reported. However, the short distance from the entrance of the flume to the joint location suggests that the boundary layer in these tests was relatively thin.

Figure 3 shows the Johnson (1976) measurements of average uplift pressures in a format that is condensed, but similar to the way they were first presented by Johnson. Uplift pressures are made dimensionless by expressing them as a percentage of the channel-average velocity head. Johnson originally showed data for each gap width on a separate plot, with individual hand-drawn curves passing through the data points collected at each velocity setting. In this condensed presentation Figure 3 shows power curves through the data for each gap width to illustrate general trends in the data. Johnson's observations highlighted previously are apparent, especially the significant increase in uplift pressure as the width of the joint gap was reduced. Although the data are not included here, trends in the 95-percent maximum uplift pressure data were similar, with the 95-percent maximum uplift typically being about 1.15 to 1.40 times the average uplift.

Water Tunnel Tests

The second significant study of the uplift pressure phenomenon was conducted at Reclamation by the second author (Frizell 2007) using a high-head pump to deliver high-velocity flow to a pressurized water tunnel containing an idealized spillway joint that could be adjusted to create offset heights of 3.2, 6.4, 12.7, and 19.1 mm ($\frac{1}{8}$, $\frac{1}{4}$, $\frac{1}{2}$, and $\frac{3}{4}$ inches) and gap widths of 3.2, 6.4, and 12.7 mm ($\frac{1}{8}$, $\frac{1}{4}$, and $\frac{1}{2}$ inch). The layout of the test facility is shown in Figure 4, with the test section located downstream from a tee on the pump discharge line. The tests could be conducted with flow velocities of about 5.2 to 14.6 m/s (17 to 48 ft/s) in the 102-mm wide by

102-mm tall (4-inch by 4-inch) section approaching the offset (Figure 5). The exit height of the test section was reduced from the nominal 102-mm (4-inch) dimension by the height of the offset. In addition to the tests with rectangular sharp-edged joint geometries, tests were also performed on joint openings with 3.2-mm by 3.2-mm ($\frac{1}{8}$ -inch by $\frac{1}{8}$ -inch) 45° chamfered edges and 3.2-mm ($\frac{1}{8}$ -inch) radius edges. Tests were conducted in a sealed configuration, where no flow could exit the chamber beneath the spillway joint, and a vented condition in which flow could exit through a valve. The size of the exit valve was not reported, but its flow capacity was not enough to keep the chamber fully vented. As a result, back pressure existed below the spillway joint in the vented tests, but it was not directly measured. Uplift pressures were measured with a differential pressure transducer connected to taps above and below the movable downstream block (Figure 6). Particle Image Velocimetry (PIV) was also used to map velocity fields above and within the joint for a small subset of the tests (chamfer-edged joints with 3-mm [$\frac{1}{8}$ -inch] and 13-mm [$\frac{1}{2}$ -inch] gap widths and 13-mm [$\frac{1}{2}$ -inch] offset heights). Finally, accompanying computational fluid dynamics (CFD) models were configured and run using the FLOW-3D software package developed by Flow Science, Inc. CFD models were created to simulate both the test facility and a prototype spillway joint. The PIV measurements and CFD models were used primarily to visualize the flow field in the vicinity of the joints. There is potential for CFD studies to be used to study uplift pressures, but quantitative uplift pressure results were not provided in this study.

The collected uplift pressure data were originally presented by Frizell (2007) in plots showing the raw differential pressures versus the average velocity over the offset (at section 2 in Figure 6). These plots verified that uplift pressure was proportional to the square of the velocity and that uplift pressures also increased with increasing offset height, but the data were not presented in a dimensionless manner that would allow direct comparison to the Johnson (1976) results. The uplift pressures tended to decrease in most cases with increasing gap widths, similar to the observation by Johnson (1976). Frizell (2007) also observed that boundary layer effects could have a substantial impact in a prototype, but made no analysis of the boundary layer conditions that existed in the tests, presuming that the boundary layer was thin and that uplift pressures would be related to the mean velocities. The tests of chamfered-edged and radius-edged joint openings showed similar trends as the tests of sharp-edged openings, with a tendency for the chamfered- and radius-edged openings to behave like sharp-edged openings of a slightly larger dimension.

In the water tunnel experiments Frizell (2007) employed a differential pressure transducer connected to piezometer taps below and above the downstream slab and reported that differential pressure as the uplift pressure. However, the use of the water tunnel causes three effects that distort this measure of uplift pressure. First, there is an increase in velocity head from the section upstream from the joint (section 1 in Figure 6) to the section downstream from the offset (section 2) due to the reduced height of the tunnel caused by the vertical offset. The lower velocity head at section 1 will be accompanied by a higher pressure head than that at section 2. The pressure in the sealed chamber beneath the slot should be expected to reflect this larger pressure head. Second, there is a loss of head at the offset due to the minor loss created by the contraction itself. This also causes an increase in pressure at section 1. Finally, there is also a friction loss in the water tunnel that creates an additional pressure difference between the two sections. Each of these three pressure difference contributors must be subtracted from the

measured pressure difference to determine the uplift caused by the stagnation of flow against the face of the vertical offset.

Similar head losses and flow changes occur in an open channel flow, but they affect the uplift pressure beneath the slab differently. In the supercritical flows tested by Johnson (1976), there was an increase in depth in the downstream direction as the flow passed over the offset and experienced contraction and friction losses. (In a subcritical flow, the depth would decrease in the downstream direction due to friction and contraction losses and the step-up in the channel bottom). However, there was no way for this depth increase to affect the flow upstream from the face of the offset or the uplift generated by the step, since pressure waves cannot travel upstream in supercritical flow. The conditions in the sealed chamber could only be influenced by the flow upstream from the offset. The increased downstream depth did have a small effect on the pressure above the downstream slab. Although Johnson explained that he subtracted out the flow depth when reporting the net uplift pressures, he did not definitely state whether he measured the flow depth upstream or downstream from the offset. It is presumed that the measurement was made downstream from the offset, since uplift of the downstream slab was of interest, but the difference in either case would be small (probably less than 25 mm = 1 inch).

In the water tunnel configuration the head losses and pressure changes associated with pressurized flow are substantial in comparison to the measured differential pressure heads. Unfortunately, there were no actual measurements of these head losses or the total head losses made during the tests. Therefore, estimates of each loss were calculated during the present review, and these were used to compute adjusted values of uplift pressure head that could be compared directly to the open channel data from Johnson (1976). The velocity head change was the most readily and accurately estimated, based on the cross section dimensions and offset height, and varied from about 14% to 50% of the measured differential pressure head. The contraction loss was estimated from equations for computing minor losses at abrupt concentric pipe contractions (Roberson and Crowe 1985) and ranged from 3% to 14% of the measured differential pressure head. The friction loss estimates had significant uncertainty depending on the assumed values of surface roughness in the test section, but were smaller than the other two effects, ranging from about 2% to 6% of the measured differential pressure head. The combined effects of all three components ranged from 20% to 66% of the measured differential pressure head.

Flow through Joints

The Frizell (2007) study reported flow rates through the joints in a vented condition, but a review of the data and the analysis procedures now shows that the pressure measurements used to indirectly determine the discharges did not accurately reflect actual flow rates. Future tests of flow through open joints should use calibrated, direct flow measurement methods and include measurements of the back pressure beneath the open joint. Running tests in a fully vented condition (with a much larger outlet valve) would provide an indication of the maximum flow that can occur through a joint experiencing no back pressure from the underlying foundation or drainage system.

Analysis

The IFT (2018) approach to estimating uplift pressure head for the Oroville Dam spillway was to estimate the velocity profile in the channel, specifically the velocity occurring at a distance above the channel bed equal to half of the height of an offset into the flow. The uplift pressure was then equal to the velocity head at this point in the profile. The two experimental data sets from Johnson (1976) and Frizell (2007) offer an opportunity to test this concept, but since velocity profiles were not measured in either study, the mid-height velocity must be estimated by analytical means.

In the Johnson (1976) open channel experiments it is reasonable to assume that the development of the boundary layer began at the slide gate that controlled the inflow, 1.52 m (5 ft) upstream from the simulated joint. For the Frizell (2007) water tunnel experiments, the boundary layer development can be assumed to begin at the upstream end of the square duct leading to the test section, 1.72 m (5.66 ft) upstream from the simulated joint. (The velocity was rapidly accelerating in the round-to-square transition leading to the square duct, almost tripling in a distance of 0.91 m [3 ft].) For both cases the velocity profile in the boundary layer can be estimated from (Roberson and Crowe 1985, Eq. 9-27):

$$v_y = u_* \left(5.75 \log_{10} \frac{yu_*}{\nu} + 5.56 \right) \quad (3)$$

with u_* being the shear velocity and ν being the kinematic viscosity of the fluid. In the early phase of boundary layer growth, the value of u_* is a function of the distance from the point of boundary layer initiation and is given by a set of three equations (Roberson and Crowe 1985, pp. 321-336, Eqs. 9-19 and 9-42):

$$u_* = \sqrt{\frac{\tau_0}{\rho}} \quad (4)$$

$$\tau_0 = \frac{0.058}{\sqrt[5]{\text{Re}_x}} \frac{\rho V^2}{2} \quad (5)$$

$$\text{Re}_x = \frac{Vx}{\nu} \quad (6)$$

where ρ is the fluid density and V is the mean channel velocity (the free-stream velocity outside of the boundary layer), and x is the distance from the start of boundary layer growth. This yields a straightforward way to calculate the boundary layer velocity profile as a function of the mean velocity of the flow. In addition, the thickness of the boundary layer at distance x can be estimated from (Roberson and Crowe 1985, Eq. 9-41):

$$\delta = \frac{0.37x}{\sqrt[5]{\text{Re}_x}} \quad (7)$$

Applying Eq. 7 to the Johnson (1976) tests, the boundary layer thickness at the test location varied from about 24.4 to 27.9 mm (0.96 to 1.1 inches), decreasing with increasing velocity, so the 38.1-mm (1.5-inch) offsets would have extended into the free stream flow, but offsets of

19.1 mm (0.75 inches) or less would have been fully contained in the boundary layer. For the Frizell (2007) tests, the boundary layer thickness varied from about 21.4 to 26.1 mm (0.84 to 1.03 inches), which is larger than all of the tested offset heights.

Johnson (1976) analyzed the uplift pressure head as a dimensionless percentage of the mean-channel velocity head, but related it to dimensional offset heights and gap widths of the tested joints. Frizell (2007) plotted the dimensional uplift pressure head versus the mean flow velocity for different offset heights and gap widths. To generalize the results in a more useful way, Figure 7 presents both sets of data plotted using a fully dimensionless approach. This figure includes the data for all gap widths, offset heights, and velocities tested by Johnson (1976) and all of the sealed-cavity, sharp-edged joint tests conducted by Frizell (2007). The average uplift pressure heads are presented as percentages of the stagnation pressure computed for the estimated boundary layer velocity at the mid-height of the offset, computed using equations 3-6. The dimensionless uplift pressures are plotted as a function of the dimensionless ratio of gap width to offset height, with the data subdivided by distinct values of offset height. This presentation collapses the data more effectively than Figure 3, indicating that uplift pressures approach 100% of the mid-height boundary layer velocity head as the ratio of gap width to offset height is reduced toward zero. The plots show clearly that there is a reduction in the developed uplift pressure for relatively wide gap width to offset height ratios, in contrast to the IFT (2018) assumption that the uplift pressure would be equal to the velocity head at mid-height of the offset, independent of the gap width dimension. The plots show that there was some dependence in the experiments on the dimensional offset height, with the data following somewhat higher curves for smaller offsets, especially the open channel data. In general, the water tunnel data exhibit slightly larger dimensionless uplift values at low gap to offset ratios and smaller values at high ratios. These differences could be due to several factors, including viscous (Reynolds) scale effects, uncertainties in the estimates of boundary layer velocity profiles, or uncertainties related to the uplift pressure adjustments applied to the water tunnel data. A curve fit to the combined data from both studies (Figure 8) produces Equation 8 with an R^2 value of 0.68, which can be used to predict the uplift pressure head:

$$\frac{H_u}{V_{bl}^2/(2g)} = e^{0.055-0.417\sqrt{\beta}} \quad (8)$$

H_u is the uplift pressure head, V_{bl} is the boundary layer velocity at the mid-height of the offset, and β is the gap width to offset height ratio.

In Figure 9 the uplift pressures are presented in a different dimensionless manner, as percentages of the velocity head computed from the channel-average velocity approaching the simulated joint. This collapses the data from each study into a single curve for all tested gap widths and offset heights. In Figure 10 the data sets are combined and a single curve fit equation is obtained with an R^2 value of 0.90:

$$\frac{H_u}{V^2/(2g)} = e^{-0.215-0.679\sqrt{\beta}} \quad (9)$$

The variables here are the same as in Eq. 8, except that V is the average velocity for the full channel. There is still a tendency at large gap width to offset height ratios for larger uplift pressures in the open channel data, but at low gap width to offset height ratios the data sets

coincide well. The better curve fit suggests that the actual boundary layer in both experiments may have been thinner than the calculated estimates, so that the uplift pressures were driven primarily by the mean-channel velocity. Eq. 9 offers a useful approach to predicting uplift pressure when there is little or no boundary layer, and is more straightforward to apply than Eq. 8 since it requires determination of only the average channel velocity instead of the more complex boundary layer velocity profile. Notably, for gap width to offset height ratios less than 0.5 the uplift pressure predicted by Eq. 9 is more than 50% of the channel-average velocity head, which exceeds the estimates of uplift pressure made by the IFT (2018) for the Oroville Dam spillway (see Table 1). To apply either Eq. 8 or 9 to a prototype case, the gap width to offset height ratio must be known, but the uplift pressure is not dependent on the actual offset height or gap width. In contrast, the IFT (2018) approach used the offset height, but did not consider any effect of the gap width. Despite these observations, one should not conclude that the magnitude of the offset height or gap width are unimportant from a practical standpoint, since large openings to the foundation should enable more flow to get beneath the slab where it can have a myriad of undesirable affects if not captured and carried away safely. Large openings should also be expected to enable uplift pressures to extend to larger areas beneath a slab.

Scale Effects

One motivation for the water tunnel tests by Frizell (2007) was the possibility of scale effects in the low-velocity open channel tests of Johnson (1976). Low velocities and Reynolds numbers might affect turbulence intensity and boundary layer development, which could in turn affect generated uplift pressures. If Reynolds number effects were present in the laboratory tests, it should be visible in a comparison of model results obtained at different Reynolds numbers. Three possible formulations of the Reynolds number could be relevant to this flow situation. The boundary layer Reynolds number is typically defined as $Re_x = Vx/\nu$ (Eq. 6), where V is the mean velocity in the channel and x is the length of the boundary layer from the start of its growth. The two other potentially useful Reynolds numbers are $Re_w = Vw/\nu$, where w is the gap width, and $Re_h = Vh/\nu$, where h is the offset height.

Frizell (2007) was able to test at velocities up to 3 times higher than those used by Johnson (1976), but the range of gap and offset Reynolds numbers for the two studies was similar, since Johnson (1976) tested larger gap widths and offsets. To test for Reynolds number effects, the data for each study were grouped within low, middle, and high ranges of the three Reynolds numbers and plots like those in Figure 7 and Figure 9 were constructed to see if different ranges of Reynolds numbers produced different curves. No consistent Reynolds number effects could be identified that were distinct from the scatter in the data.

Application and Research Needs

The Oroville Dam Independent Forensic Team did not use the results of either the Johnson (1976) or Frizell (2007) studies for prediction of uplift pressures, instead opting to assume that uplift would be equal to the stagnation pressures associated with flow velocity in the boundary layer at of the mid-height of an offset. The present study reanalyzed the Johnson (1976) and Frizell (2007) data sets to develop Eq. 8, which relates the uplift pressure to the boundary layer velocity profile, and Eq. 9 which relates the uplift pressure to the mean velocity in a channel.

Notably, both equations show that there is an important additional effect beyond that assumed by IFT (2018), namely the influence of the geometric ratio of gap width to offset height. Eq. 9 is convenient to apply since it does not require estimation of boundary layer velocities. Both equations are superior to the relations provided by the original studies, since they use dimensionless forms that do not require matching application details to a specific test run at a particular velocity, offset height, or gap width. Because Eq. 9 is based on channel-average velocity rather than boundary layer velocities, it is likely to yield conservatively high estimates of uplift pressure for long chutes in which boundary layer velocities could be much lower than average velocities.

The uncertainty of Eq. 8 is large, but it still offers potential to be valuable in prototype spillways with long chutes, since boundary layer effects could reduce uplift pressures significantly. Through its influence on the boundary layer, spillway surface roughness could be an important factor, with uniformly rough surfaces having less uplift potential than smooth surfaces. To further improve this approach to the problem, experimental data are needed from test facilities in which the boundary layer velocities are significantly different from the channel-average velocity and can be adjusted and measured. The studies by Johnson (1976) and Frizell (2007) both varied the average flow velocity significantly, but boundary layer velocities were not measured, and estimated boundary layer velocities at the mid-height of the tested offsets were typically about 70-90% of the average velocity. For comparison, for the Oroville Dam spillway the estimated boundary layer velocities underlying the stagnation pressure estimates in Table 1 ranged from about 50-70% of the average velocity.

Aerated flow is another factor that could have an important influence, both for its effect on the boundary layer and for its effect on pressure propagation through joints and resonance within joints. Aeration effects should be studied after non-aerated conditions are well understood.

This study has considered only the uplift pressures generated beneath a slab when the foundation is sealed. In real spillways, the natural or engineered means for conveying water out of the foundation and dissipating uplift pressure are also important for determining total uplift forces. To assess the removal of water from the foundation, it is necessary to estimate amounts of water entering through spillway joints or cracks. For this purpose, IFT (2018) used equations that predicted leakage rates due to piezometric pressure heads in the chute (i.e., pressure due only to the depth of flow); these equations did not reflect any increased flow that might occur due to an offset projecting into the flow. Currently there is not a good source of laboratory testing to support making estimates of flow through joints with offsets. Research should be initially focused on prediction of flow rates assuming fully vented conditions beneath the slab or partially vented conditions with measurement of the backpressure beneath the slab. For application in the field, the flow rates estimated for the fully vented condition could be modified based on a separate analysis of the underlying drainage layer or drainage system.

A potentially valuable avenue for further research on this topic is field-scale studies. To the best of the authors' knowledge, there have been no attempts to measure uplift pressures beneath the lining of prototype spillways. An instrumented prototype spillway could enable the collection of data for high-velocity flows with realistic boundary layer and aerated flow conditions.

This review was initiated with the goal of developing a research plan to address the influence of factors such as complex flow paths through spillway joints (effects of keyways, waterstops, reinforcement, etc.), variations in the openness of joints, and differences in joint configuration (vertical offsets, spalls, and joints oriented acutely to the flow). However, the review has shown that there are still fundamental issues that need to be resolved before these complexities are considered. Until the necessary research can be completed, defensive design practices and proactive maintenance programs to prevent the widespread existence of open or offset joints are crucial to defend against hydraulic jacking.

Acknowledgments

The authors appreciate the detailed comments of the three anonymous reviewers and the editor and associate editor. Their constructive criticism led to significant improvement of the paper. The data from the Johnson (1976) study were digitized from the original figures and can be obtained by e-mail request from the lead author, along with the complete data set from the Frizell (2007) study. The authors wish to especially acknowledge the work of the late Perry Johnson who inspired us all and continues to do so today.

This work was jointly funded by Reclamation's Science & Technology Program and Dam Safety Technology Development Program.

Notation

H_u = uplift pressure head

ΔP = Pressure difference between chamber below slab and water tunnel flow above slab

P_s = stagnation pressure

Q_{joint} = flow rate through spillway joint

$Q_{spillway}$ = flow over slab downstream from offset joint

Q_{total} = total flow approaching offset in water tunnel test facility

Re_x = boundary layer Reynolds number based on mean velocity and distance from start of boundary layer growth, $Re_x = Vx/\nu$

Re_w = Reynolds number based on mean velocity and gap width, $Re_w = Vw/\nu$

Re_h = Reynolds number based on mean velocity and offset height, $Re_h = Vh/\nu$

V = mean flow velocity approaching a spillway joint

V_{bl} = boundary layer velocity at mid-height of an offset

e = base of natural logarithms, 2.7183

f = Darcy-Weisbach friction factor

g = acceleration due to gravity

h = offset height

u_* = shear velocity

v_y = velocity at distance y above the boundary, approach velocity of the stagnated flow

w = gap width

x = distance from start of boundary layer growth

y = distance from the boundary

y_0 = total flow depth

β = ratio of gap width to offset height

γ = unit weight of water

δ = boundary layer thickness

ρ = fluid density

τ_0 = bed shear stress

ν = kinematic viscosity

References

- Barjastehmaleki, S., V. Fiorotto, and E. Caroni, 2016a. Spillway stilling basins lining design via Taylor hypothesis. *Journal of Hydraulic Engineering*, 142(6).
- Barjastehmaleki, S., V. Fiorotto, and E. Caroni, 2016b. Design of stilling basin linings with sealed and unsealed joints. *Journal of Hydraulic Engineering*, 142(12).
- Bellin, A. and V. Fiorotto 1995. Direct dynamic force measurement on slabs in spillway stilling basins. *Journal of Hydraulic Engineering*, 121(10):686-693.
[https://doi.org/10.1061/\(ASCE\)0733-9429\(1995\)121:10\(686\)](https://doi.org/10.1061/(ASCE)0733-9429(1995)121:10(686))
- Bollaert, E. and A. Schleiss, 2003a. Scour of rock due to the impact of plunging high velocity jets, Part I: A state-of-the-art review, *Journal of Hydraulic Research*, 41(5):451-464, DOI: [10.1080/00221680309499992](https://doi.org/10.1080/00221680309499992)
- Bollaert, E. and A. Schleiss, 2003b. Scour of rock due to the impact of plunging high velocity jets, Part II: Experimental results of dynamic pressures at pool bottoms and in one- and two-dimensional closed end rock joints, *Journal of Hydraulic Research*, 41(5):465-480, DOI: [10.1080/00221680309499992](https://doi.org/10.1080/00221680309499992)
- Bollaert, E., and A. Schleiss, 2005. Physically based model for evaluation of rock scour due to high-velocity jet impact. *Journal of Hydraulic Engineering*, 131(3):153-165.
[https://doi.org/10.1061/\(ASCE\)0733-9429\(2005\)131:3\(153\)](https://doi.org/10.1061/(ASCE)0733-9429(2005)131:3(153))
- Bowers, C.E. and J. Toso, 1988. Karnafuli Project, model studies of spillway damage. *Journal of Hydraulic Engineering*, 114(5). [https://doi.org/10.1061/\(ASCE\)0733-9429\(1988\)114:5\(469\)](https://doi.org/10.1061/(ASCE)0733-9429(1988)114:5(469))
- Bureau of Reclamation, 2014. Design Standards No. 14, Appurtenant Structures for Dams (Spillways and Outlet Works), Chapter 3: General Spillway Design Considerations, Section 3.8.6. <https://www.usbr.gov/tsc/techreferences/designstandards-datacollectionguides/finalds-pdfs/DS14-3.pdf>
- Dong, Z., Wu, Y., and Zhang, D., 2010. Cavitation characteristics of offset-into-flow and effect of aeration, *Journal of Hydraulic Research*, 48(1):74-80, DOI:10.1080/00221680903566083
- Falvey, H.T. 1990. *Cavitation in Chutes and Spillways*, Engineering Monograph 42, U.S. Dept. of the Interior, Bureau of Reclamation, Denver, CO.
- Fiorotto, V. and A. Rinaldo 1992a. Fluctuating uplift and lining design in spillway stilling basins. *Journal of Hydraulic Engineering*, 118(4). [https://doi.org/10.1061/\(ASCE\)0733-9429\(1992\)118:4\(578\)](https://doi.org/10.1061/(ASCE)0733-9429(1992)118:4(578))

- Fiorotto, V. and A. Rinaldo, 1992b. Turbulent pressure fluctuations under hydraulic jumps. *Journal of Hydraulic Research*, 30(4):499-520. <https://doi.org/10.1080/00221689209498897>
- Fiorotto, V. and P. Salandin, 2000. Design of anchored slabs in stilling basins. *Journal of Hydraulic Engineering*, 126(7):502-512. [https://doi.org/10.1061/\(ASCE\)0733-9429\(2000\)126:7\(502\)](https://doi.org/10.1061/(ASCE)0733-9429(2000)126:7(502))
- Fiorotto, V. and E. Caroni, 2014. Unsteady seepage applied to lining design in stilling basins. *Journal of Hydraulic Engineering*, 140(7).
- Frizell, K.W., 2007. *Uplift and Crack Flow Resulting from High Velocity Discharges over Open Offset Joints*. Report DSO-07-07, Bureau of Reclamation Dam Safety Technology Development Program, Denver, CO. https://www.usbr.gov/tsc/techreferences/hydraulics_lab/pubs/DSO/DSO-07-07.pdf
- González-Betancourt, M. and L. Posada-García, 2016. Effects of joints and their waterstops on pressures spread over a slab. *DYNA* 83(197):94-103. <http://dx.doi.org/10.15446/dyna.v83n197.47579>
- Hepler, T.E., and P.L. Johnson, 1988. Analysis of spillway failures by uplift pressure. In: *Hydraulic Engineering*, Proceedings of the 1988 National Conference on Hydraulic Engineering and International Symposium on Model-Prototype Correlations, ASCE, Colorado Springs, Colorado, Aug. 8-12, 1988. S.R. Abt and J. Gessler, editors. <http://cedb.asce.org/CEDBsearch/record.jsp?dockkey=0057459>
- IFT, 2018. *Independent Forensic Team Report: Oroville Dam Spillway Incident*, January 5, 2018. [https://damsafety.org/sites/default/files/files/Independent Forensic Team Report Final 01-05-18.pdf](https://damsafety.org/sites/default/files/files/Independent%20Forensic%20Team%20Report%20Final%2001-05-18.pdf)
- Johnson, P.L., 1976. Research into uplift on steep chute lateral linings. Memorandum to the Open and Closed Conduit Systems Committee, Bureau of Reclamation, Denver CO. https://www.usbr.gov/tsc/techreferences/hydraulics_lab/pubs/PAP/PAP-1163.pdf
- Liu, P.Q., and A.H. Li, 2007. Model discussion of pressure fluctuations propagation within lining slab joints in stilling basins. *Journal of Hydraulic Engineering*, 133(6):618-624. [https://doi.org/10.1061/\(ASCE\)0733-9429\(2007\)133:6\(618\)](https://doi.org/10.1061/(ASCE)0733-9429(2007)133:6(618))
- Mahzari, M., and A.J. Schleiss, 2010. Dynamic analysis of anchored concrete linings of plunge pools loaded by high velocity jet impacts issuing from dam spillways. *Dam Engineering*, 20(4):307-327.
- Melo, J.F., A.N. Pinheiro, and C.M. Ramos, 2006. Forces on plunge pool slabs: influence of joints location and width. *Journal of Hydraulic Engineering*, 132(1):49-60. [https://doi.org/10.1061/\(ASCE\)0733-9429\(2006\)132:1\(49\)](https://doi.org/10.1061/(ASCE)0733-9429(2006)132:1(49))
- Pells, S., 2016. Erosion of rock in spillways. Doctoral thesis, University of New South Wales, School of Civil and Environmental Engineering.

https://www.unswworks.unsw.edu.au/primo-explore/fulldisplay?docid=unsworks_39826&context=L&vid=UNSWORKS&lang=en_US

Roberson, J.A., and C.T. Crowe, 1985. *Engineering Fluid Mechanics*, 3rd ed., Houghton Mifflin Company, Boston, MA.

Rouse, H., 1945. *Elementary Mechanics of Fluids*. John Wiley & Sons, p. 199.

Toso, J.W., and C.E. Bowers, 1988. Extreme pressures in hydraulic-jump stilling basins. *Journal of Hydraulic Engineering*, 114(8). [https://doi.org/10.1061/\(ASCE\)0733-9429\(1988\)114:8\(829\)](https://doi.org/10.1061/(ASCE)0733-9429(1988)114:8(829))

Trojanowski, J., 2004. Assessing failure potential of spillways on soil foundation. Association of State Dam Safety Officials Annual Conference, Lexington, KY.

Trojanowski, J., 2008. DAM SAFETY: Evaluating Spillway Condition, *Hydro Review*, Vol. 27, Issue 2, April 2008. <https://www.hydroworld.com/articles/hr/print/volume-27/issue-2/technical-articles/dam-safety-evaluating-spillway-condition.html>

Wahl, T.L, K.W. Frizell, and H.T. Falvey, 2019. *SpillwayPro – Tools for Analysis of Spillway Cavitation and Design of Chute Aerators*, Hydraulic Laboratory Report HL-2019-03, U.S. Dept. of the Interior, Bureau of Reclamation, Denver, CO.

Tables

Table 1. — Stagnation pressures at Sta. 1006 m (33+00 ft) of the Oroville Dam spillway, at half of the offset height for three hypothetical offsets.

Discharge (m ³ /s)	Flow depth (m)	Average velocity (m/s)	Average velocity head (m)	Darcy- Weisbach friction factor, <i>f</i>	Stagnation pressure head at 50% of offset height (m) (and as % of channel-average velocity head)		
					6-mm offset	12-mm offset	25-mm offset
850	0.60	26.1	34.6	0.0132	11.3 (33%)	14.3 (41%)	17.7 (51%)
1530	0.94	30.0	46.0	0.0121	13.8 (30%)	17.3 (38%)	21.5 (47%)

Source: Adapted from IFT (2018, Appendix B, Table 2).

Note: Errors in the original table are corrected and pressures are provided in SI units and as percentages of channel-average velocity head.

Figures

Figure 1. — Spillway damage observed after gates were initially closed at midday, February 7, 2017 (DWR photo; reprinted from IFT 2018, with permission).

Figure 2. — Ultimate damage at the Oroville Dam service spillway in May 2017 (DWR photo; reprinted from IFT 2018, with permission).

Figure 3. — Johnson (1976) data on uplift pressures in sealed offset joints, as originally presented in the form of percentages of the channel-average velocity head versus offset height. Power curve trend lines for each gap width are for illustration only; Johnson (1976) drew individual curves by hand through the data points for each gap width and velocity setting.

Figure 4. — Plan view of test facility setup showing pump, piping, flow meter, and test section. The 2.44-m (8-ft) long approach to the test section consisted of a 0.91-m (3-ft) long round-to-square transition (191-mm [7.5-inch] diameter to 102-mm [4-inch] square), followed by 1.52 m (5 ft) of 102-mm (4-inch) square duct. (Adapted from Frizell 2007)

Figure 5. — Test chamber used by Frizell (2007). The upstream round-to-square transition is not yet attached in this photo. The thickness of the upstream slab is 25.4 mm (1 inch). (Adapted from Frizell 2007)

Figure 6. — Test apparatus and location of pressure taps for uplift pressure measurement (Adapted from Frizell 2007).

Figure 7. — Uplift pressure head as a percentage of boundary layer velocity head related to joint geometry.

Figure 8. — Curve relating uplift pressure head to boundary layer velocity and the gap width to offset height ratio.

Figure 9. — Uplift pressure head as a percentage of mean-channel velocity head, related to joint geometry.

Figure 10. — Curve relating uplift pressure head to channel-mean velocity and the gap width to offset height ratio.

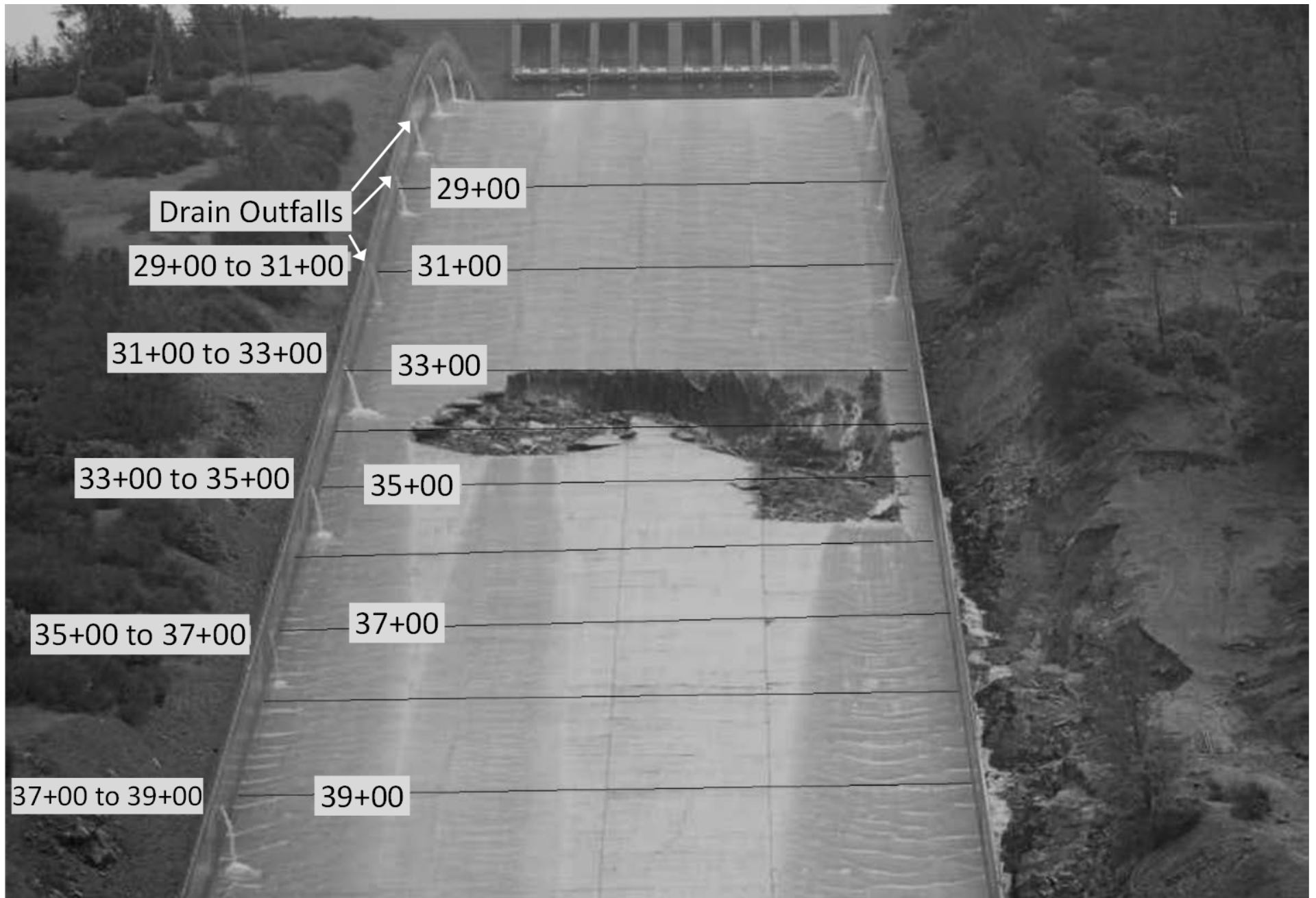


Figure 1. — Spillway damage observed after gates were initially closed at midday, February 7, 2017 (DWR photo; reprinted from IFT 2018, with permission).



Figure 2. — Ultimate damage at the Oroville Dam service spillway in May 2017 (DWR photo; reprinted from IFT 2018, with permission).

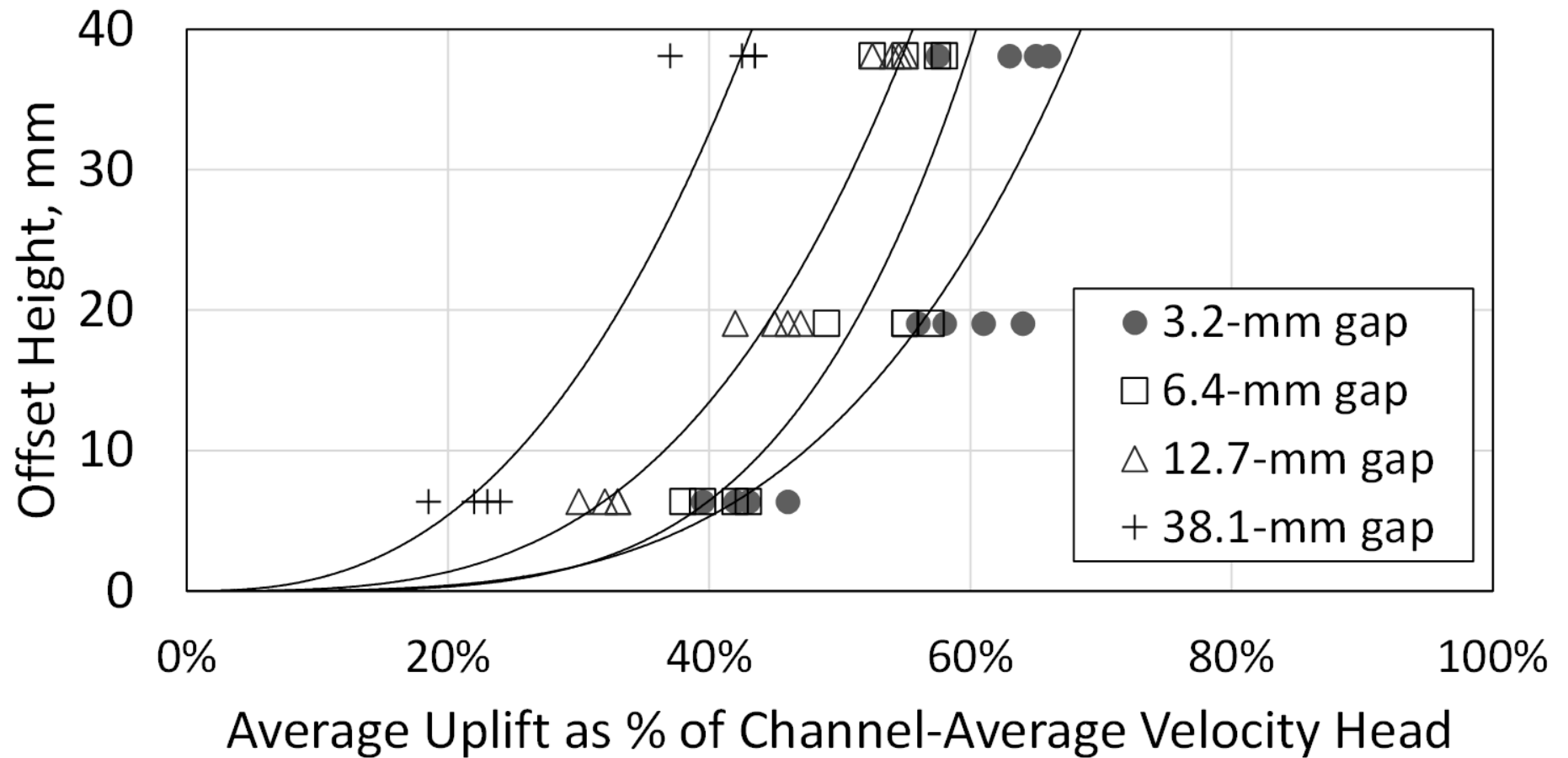


Figure 3. — Johnson (1976) data on uplift pressures in sealed offset joints, as originally presented in the form of percentages of the channel-average velocity head versus offset height. Power curve trend lines for each gap width are for illustration only; Johnson (1976) drew individual curves by hand through the data points for each gap width and velocity setting.

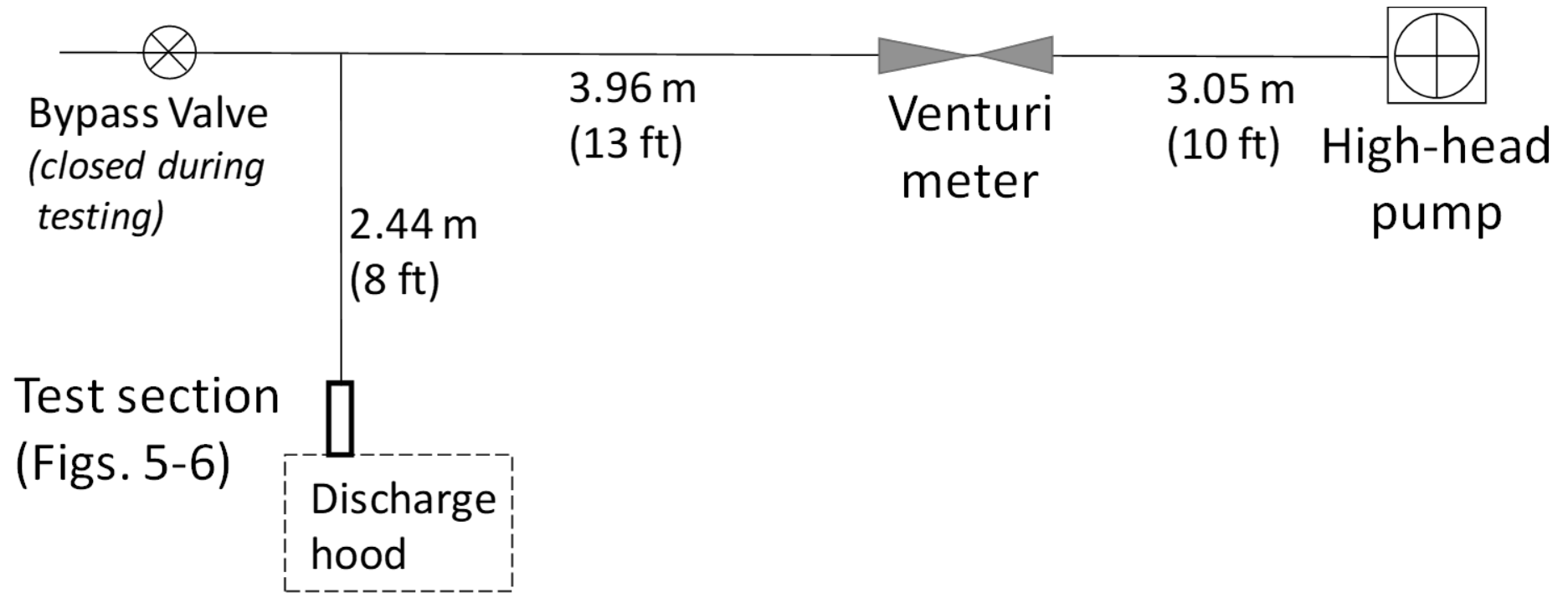


Figure 4. — Plan view of test facility setup showing pump, piping, flow meter, and test section. The 2.44-m (8-ft) long approach to the test section consisted of a 0.91-m (3-ft) long round-to-square transition (191-mm [7.5-inch] diameter to 102-mm [4-inch] square), followed by 1.52 m (5 ft) of 102-mm (4-inch) square duct. (Adapted from Frizell 2007)

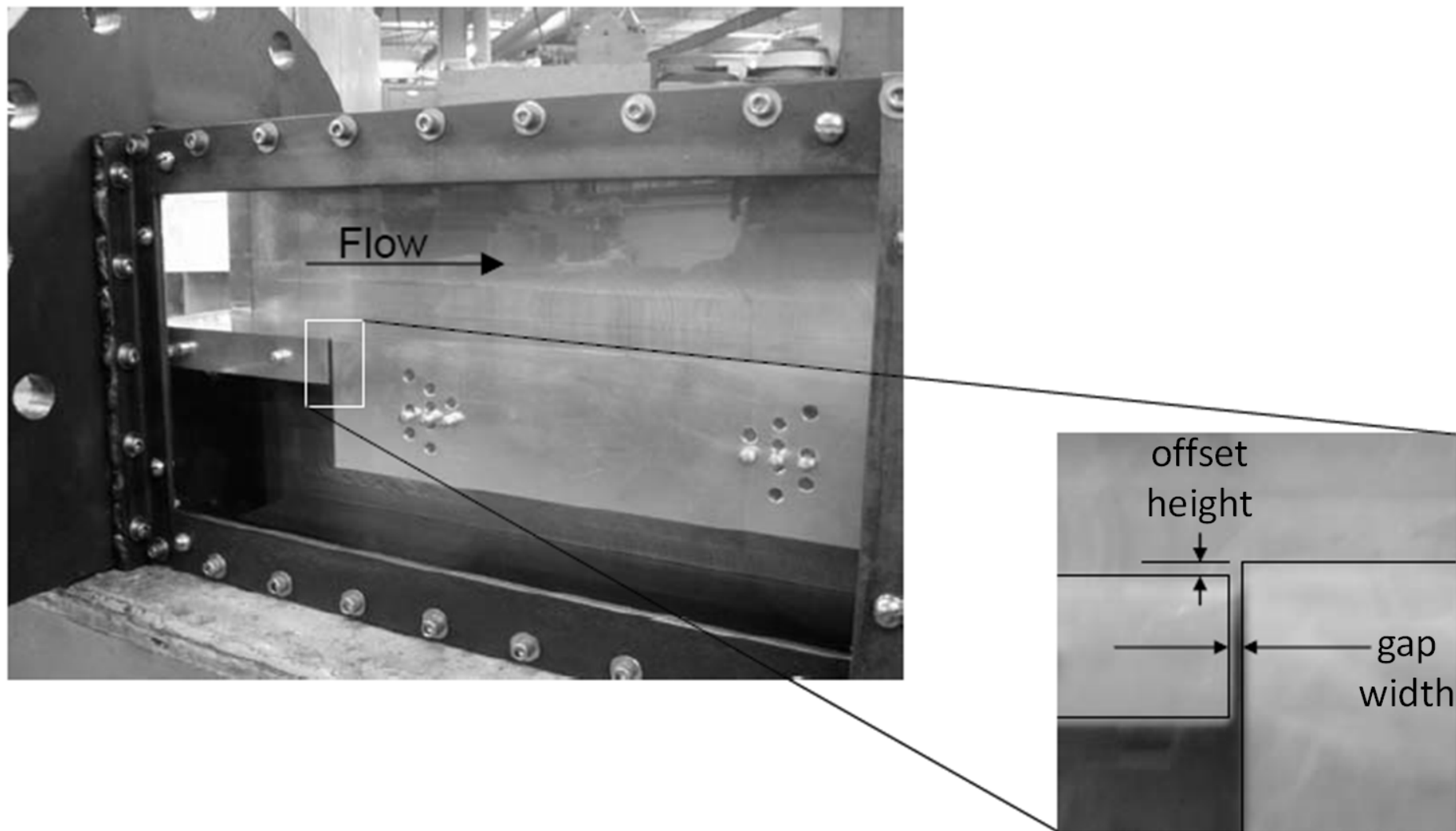
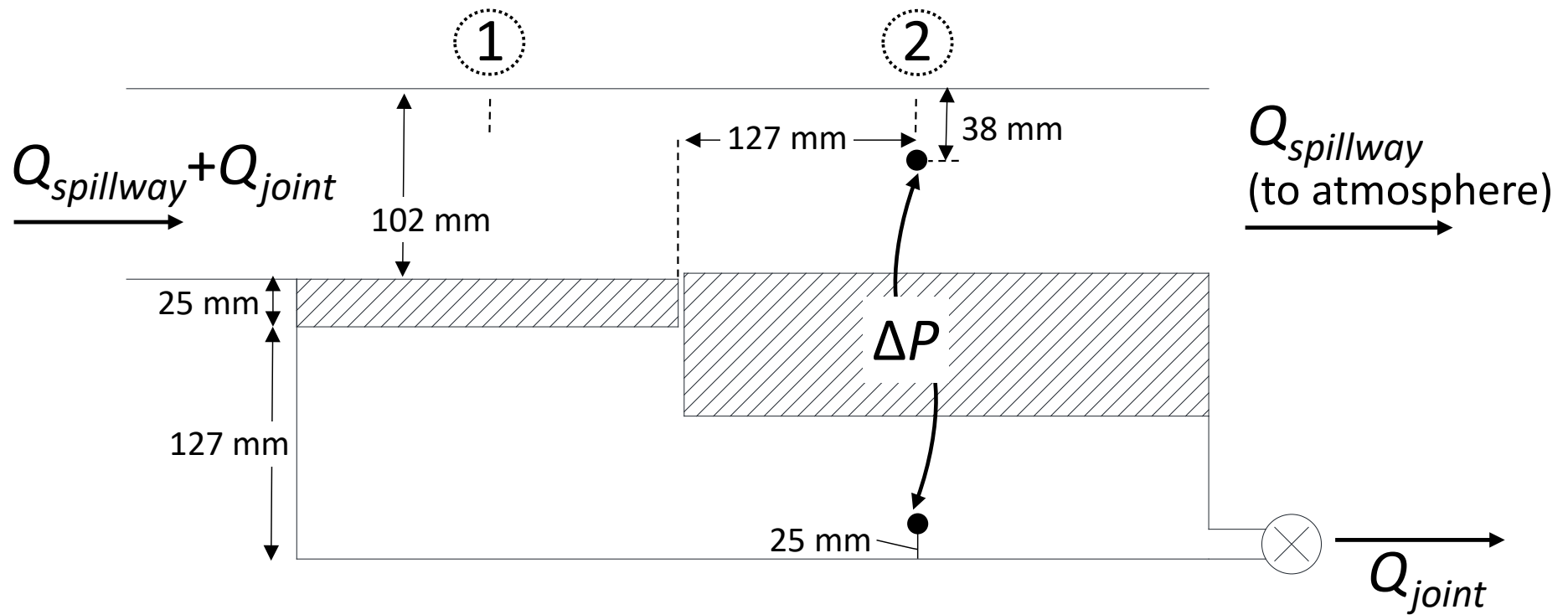


Figure 5. — Test chamber used by Frizell (2007). The upstream round-to-square transition is not yet attached in this photo. The thickness of the upstream slab is 25.4 mm (1 inch). (Adapted from Frizell 2007)



Uplift pressure, ΔP , measured by differential transducer across indicated taps

Figure 6. — Test apparatus and location of pressure taps for uplift pressure measurement (Adapted from Frizell 2007).

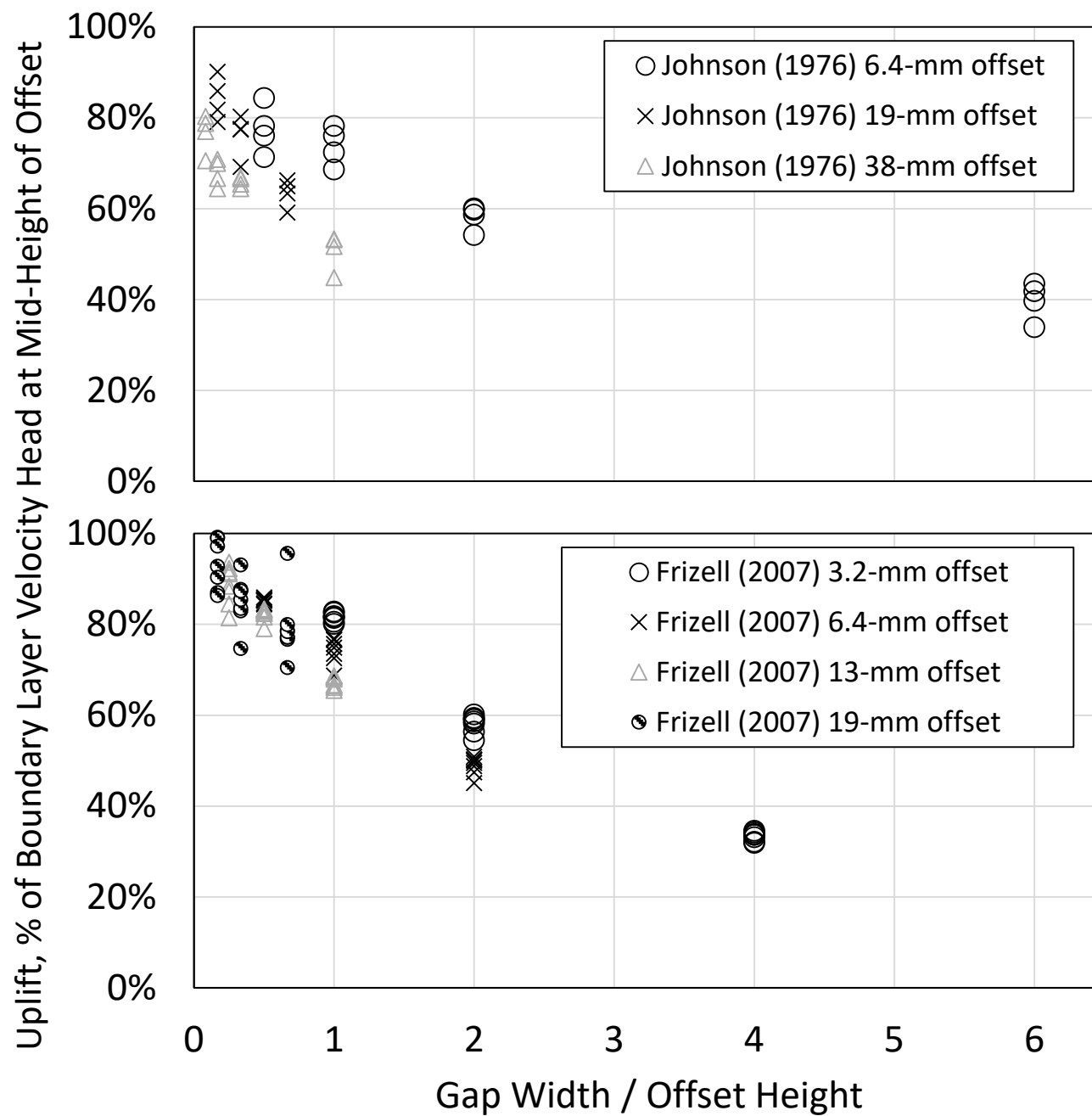


Figure 7. — Uplift pressure head as a percentage of boundary layer velocity head related to joint geometry.

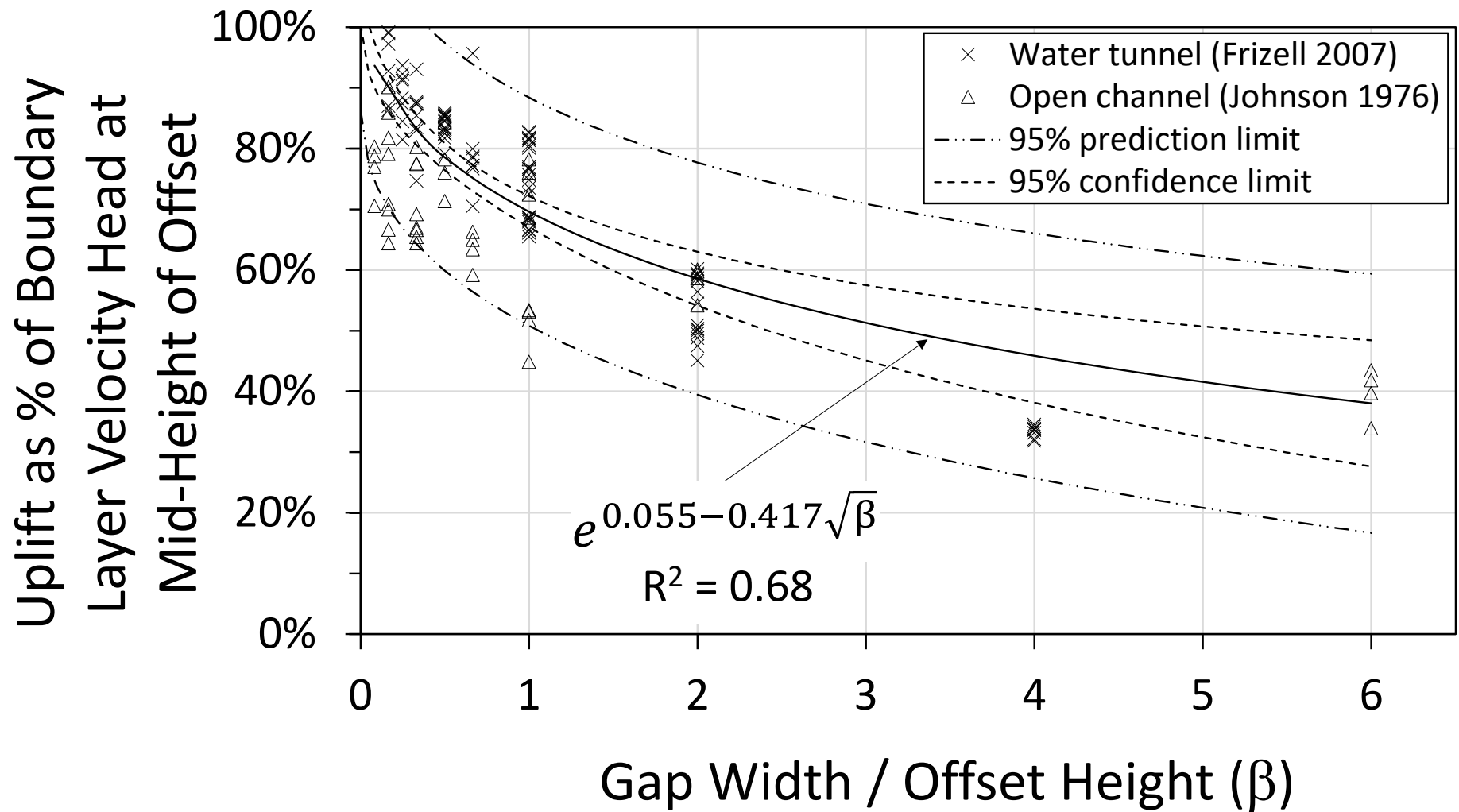


Figure 8. — Curve relating uplift pressure head to boundary layer velocity and the gap width to offset height ratio.

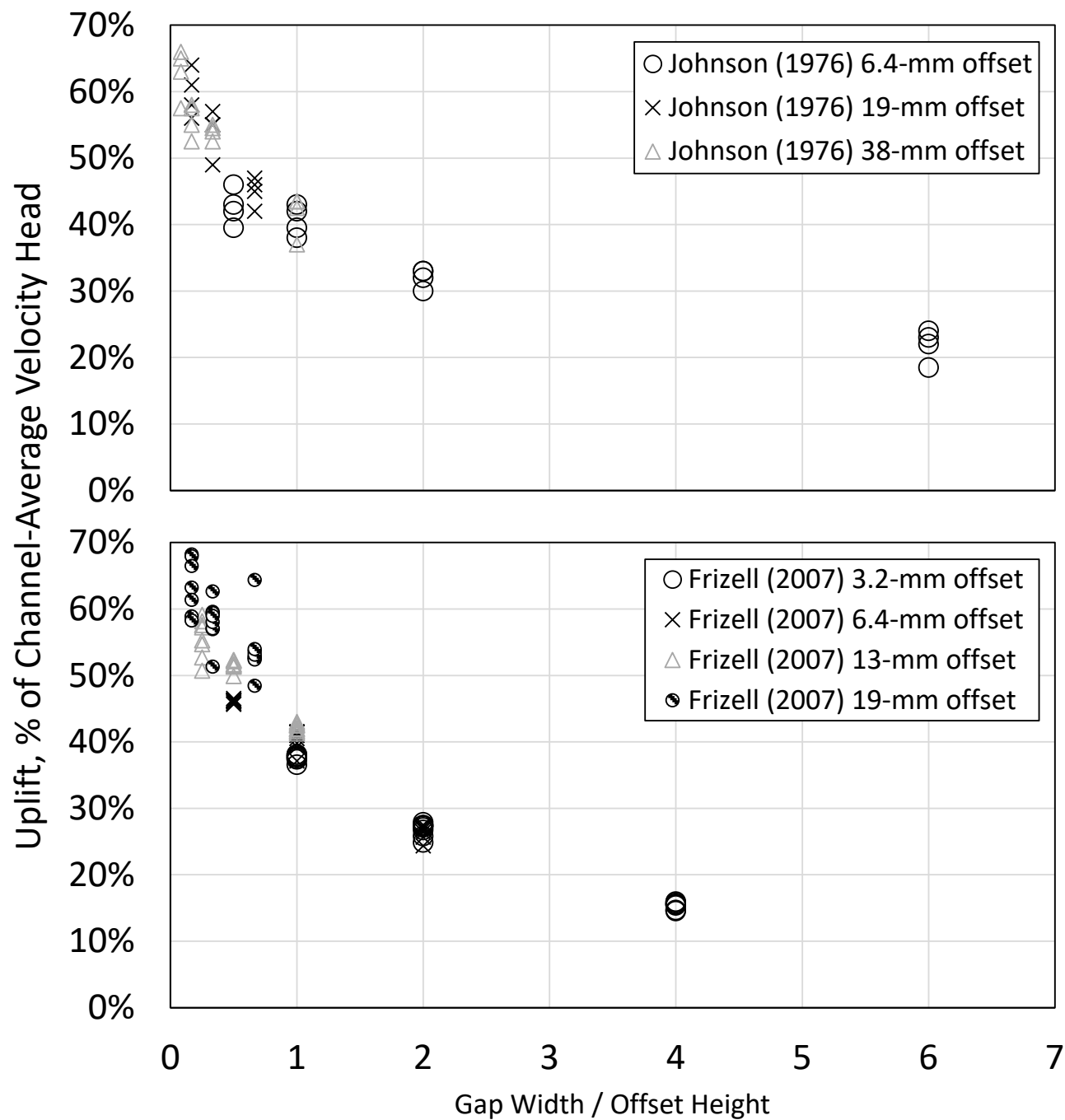


Figure 9. — Uplift pressure head as a percentage of mean-channel velocity head, related to joint geometry.

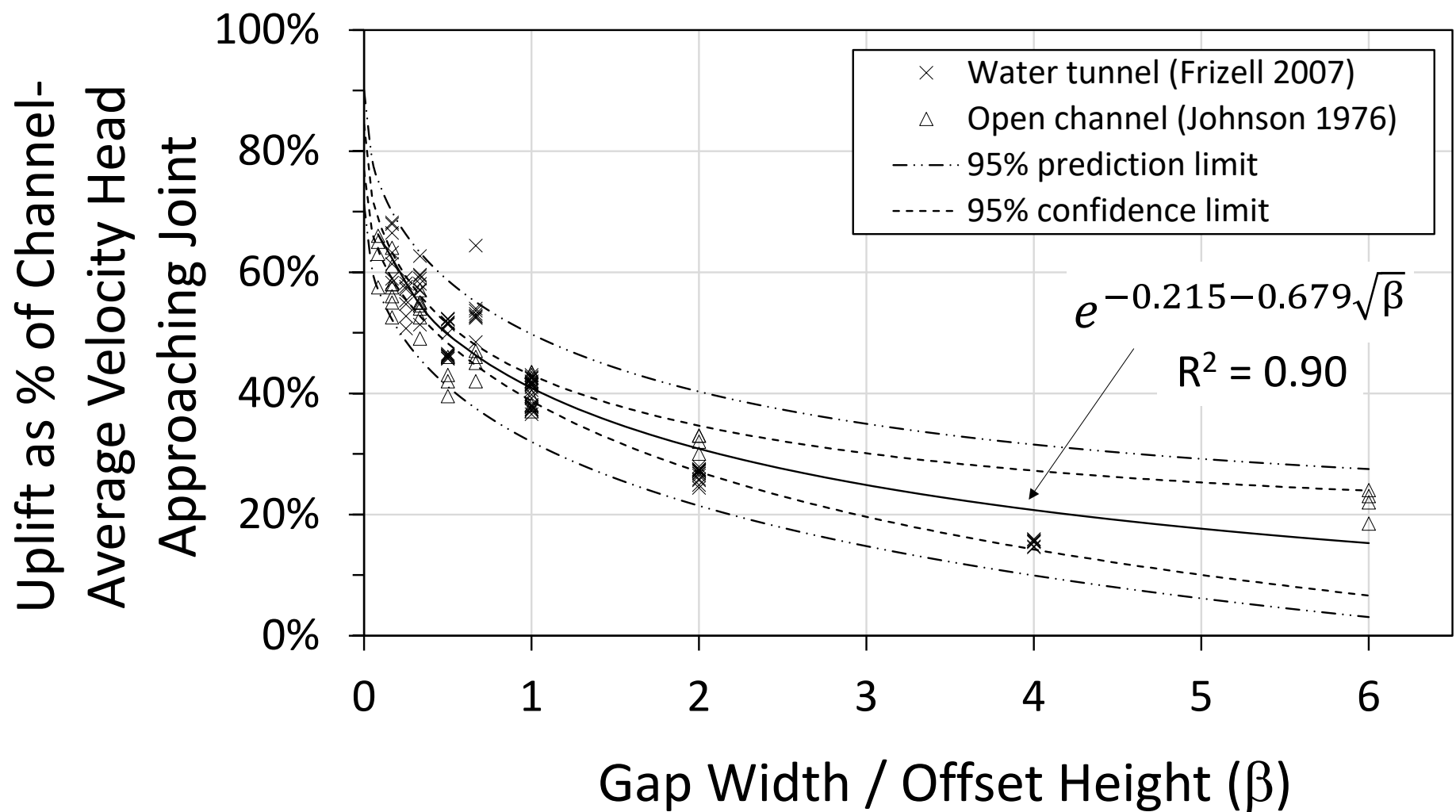


Figure 10. — Curve relating uplift pressure head to channel-mean velocity and the gap width to offset height ratio.

Appendix B

A manuscript containing a historical review and discussion of the physical significance of the roughness Froude number (related to a similar parameter correlated to the uplift pressures measured during this study) was submitted on August 9, 2021 to a refereed journal, the *Journal of Hydraulic Research* (International Association for Hydro-Environment Engineering and Research, IAHR). The principal investigator will update this section to include the submitted manuscript once the journal peer review process has been completed and information is ready for public dissemination.

